

AN ABSTRACT OF THE THESIS OF

Nancy Ann Brewster for the degree of Master of Science

in Oceanography presented on April 21, 1977

Title: CENOZOIC BIOGENIC SILICA SEDIMENTATION IN THE
ANTARCTIC OCEAN, BASED ON TWO DEEP SEA DRILLING
PROJECT SITES.

Abstract approved:



Tjeerd H. van Andel

The Antarctic Ocean during the Cenozoic experienced four periods of increased surface productivity: the Middle Eocene; the beginning of the Miocene; the Middle Miocene; and near the Miocene-Pliocene boundary. The fourth increase in productivity began five million years ago and has since progressively increased to the present level of intense surface productivity.

The major control of Antarctic surface productivity is climate. Opal production in the Neogene increased during glacial times, due to the intensification of upwelling south of the Polar Front, caused from accelerated atmospheric circulation and an increased volume production of Antarctic Bottom Water. Cenozoic variations in surface productivity are also related to the tectonic changes in the Antarctic Ocean basin, which altered the patterns of surface and thermohaline

circulation. Antarctic Surface Waters became more conducive to biological productivity with the progressive latitudinal and thermal isolation of Antarctica. The efficiency of surface productivity has progressed to such an extent that much of the global silica supply has been transferred to the Antarctic at the expense of other productive oceanic regions such as the Central Equatorial Pacific.

In the Neogene, the preservation or dissolution of calcium carbonate is influenced by the rate of upwelling south of the Polar Front. During glacial times, the upwelling of CO₂-rich Circumpolar Deep Water accelerates and effectively raises the calcite compensation depth.

Cenozoic Biogenic Silica Sedimentation in the
Antarctic Ocean, Based on Two Deep
Sea Drilling Project Sites

by

Nancy Ann Brewster

A THESIS

submitted to

Oregon State University

in partial fulfillment of
the requirements for the
degree of

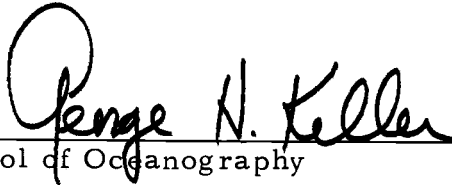
Master of Science

Commencement June 1977

APPROVED:



Professor of Oceanography
in charge of major



Dean of School of Oceanography



Dean of Graduate School

Date thesis presented April 21, 1977

ACKNOWLEDGEMENTS

I would like to thank Dr. Tjeerd van Andel, who as my major professor, offered me continuing advice and support. Thanks also go to Dr. Erwin Seuss, for his help, concern, and interest in the thesis work. Dr. Jorn Thiede offered helpful criticism and comments. The high scientific standards of these three committee members stimulated my thinking and improved the quality of the thesis.

I also acknowledge Drs. Julius Dasch and Ken Krane, for their comments, and for serving on my committee.

Discussions with J. Toth, A. Molina-Cruz, and Dr. H. Schrader contributed to the study.

P. Lawrence assisted with the drafting. Samples were provided by the Deep Sea Drilling Project. GRAPE data were provided by Peter Woodbury.

This investigation was supported by the National Science Foundation grant number OCE75-21833.

TABLE OF CONTENTS

INTRODUCTION	1
APPROACH TO OPAL DETERMINATION	11
ANALYTICAL RESULTS	15
Opal Content	15
Calcium Carbonate Content	18
Non-Biogenic Residue Content	18
Detrital Quartz Content	19
Accumulation Rates	21
Dissolution of Opal and the Opal Supply to Bottom Sediments	
TECTONIC, GLACIAL, AND PALEOCEANOGRAPHIC HISTORY OF THE SOUTHERN OCEAN	36
DISCUSSION	40
Surface Productivity and Sedimentation in the Antarctic Ocean: Eocene and Oligocene	40
Surface Productivity and Neogene Paleotemperatures	42
Calcium Carbonate Preservation	50
Surface Productivity in the Antarctic and Pacific Oceans	52
CONCLUSIONS	56
REFERENCES	58
APPENDICES	70
APPENDIX I	70
APPENDIX II	78
APPENDIX III	87
APPENDIX IV	91
APPENDIX V	95
APPENDIX VI	97

LIST OF TABLES

<u>Table</u>		<u>Page</u>
1.	Statistics of regression equation	75

LIST OF FIGURES

<u>Figure</u>		<u>Page</u>
1.	Surface and thermohaline circulation in the Antarctic Ocean, showing marine sedimentary belts.	2
2.	DSDP site locations and core descriptions.	7
3.	% Sedimentary components.	17
4.	% Clay, % Al, % Mg, % Si (clay-bound)	20
5.	Antarctic accumulation rates in the Cenozoic	22
6.	Cenozoic Pacific sedimentation and accumulation rates.	25
7.	Silica cycle in the Antarctic Ocean.	33
8.	Cenozoic paleotemperatures and opal and CaCO ₃ accumulation rates.	43
9.	Extrapolated opal production for the Antarctic and Pacific Oceans.	53
10.	Comparison of clay-bound silica, predicted and measured.	76

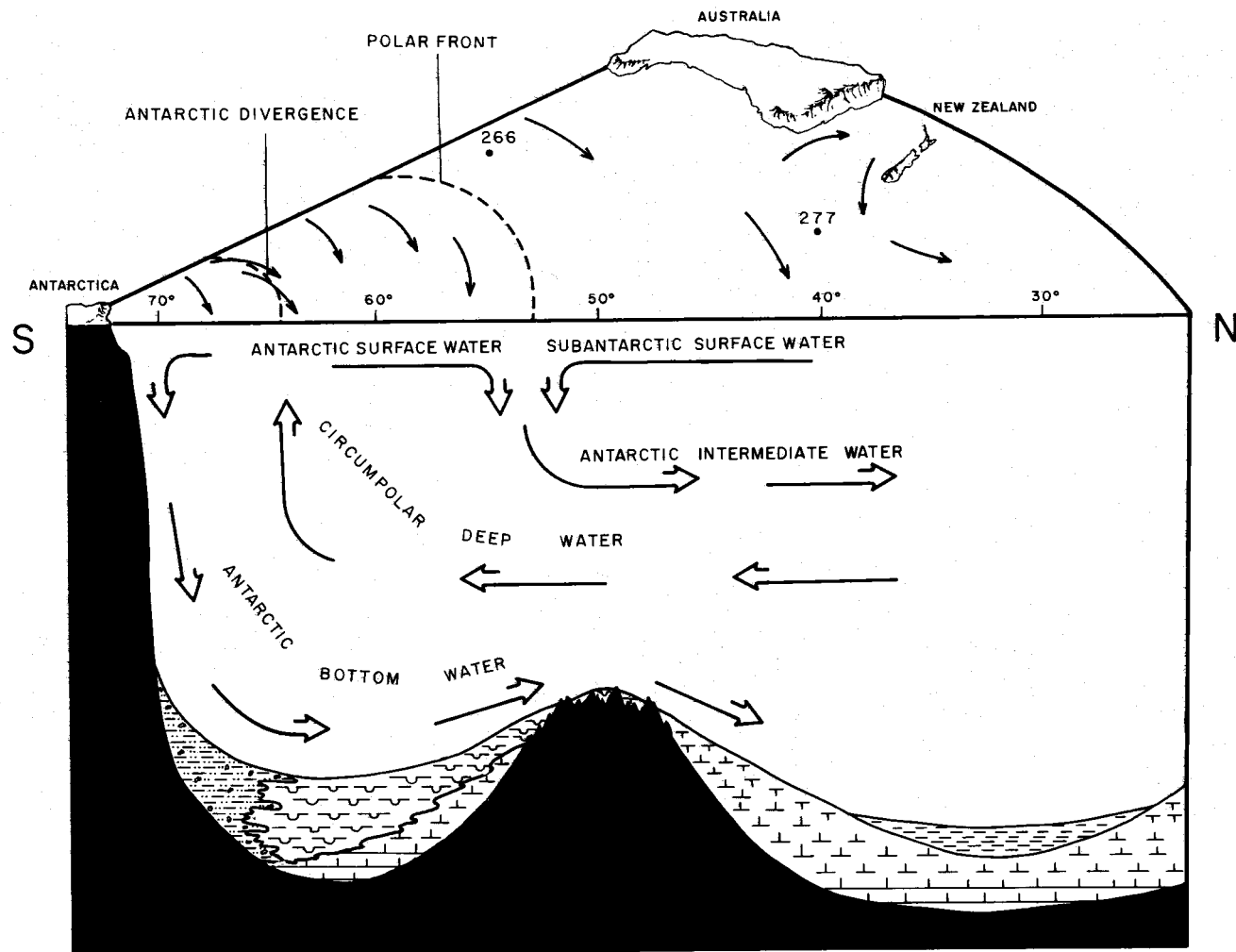
CENOZOIC BIOGENIC SILICA SEDIMENTATION IN THE ANTARCTIC OCEAN, BASED ON TWO DEEP SEA DRILLING PROJECT SITES

INTRODUCTION

The dramatic and unique marine features of today's Antarctic region have stimulated the interest of paleoceanographers. The dominating feature of the region is the Circum-Antarctic Current, circling the continent from west to east at about 50° south latitude, mixing, cooling, and oxygenating waters from all oceans. The circumpolar current transports 200 million cubic meters of water per second, with deep-seated flow that is felt throughout the water column to the seafloor (Gordon, 1971b; Callahan, 1971).

Gordon (1971a; 1971b) has shown the Southern Ocean to be the driving force of thermohaline circulation of all oceans. This is primarily due to the Antarctic Bottom Water (AABW) which forms from a combination of cooling of Antarctic surface water and seasonal freezing of sea and shelf ice near the Antarctic continent. This dense, cold, hypersaline AABW penetrates far north into the world's major ocean basins, where it eventually undergoes mixing, and returns to the Antarctic as part of a deep water mass flow (Figure 1).

The Antarctic Convergence, or more aptly, the Polar Front, situated at about 55° south, marks the boundary between the Antarctic and Subantarctic surface water masses. Antarctic Surface Water is



BR EWSTER

Figure 1. Cartoon illustrating surface and thermohaline circulation in the Antarctic Ocean, after Gordon (1971b). Latitudinal zonation of bottom sediments is shown. Glacial pebbly silts lie near Antarctica, and are succeeded to the north by diatom ooze and clay. North of this lies a belt of foram-nanno ooze, and at depths below the CCD, clay.

cold and nutrient-rich and supports a rich planktonic assemblage dominated by diatoms (Lisitzin, 1967; 1962). Ice rafting occurs in Antarctic Surface Water near the Antarctic continent. Subantarctic Surface Water is warmer, and much lower in nutrient content and carries a predominantly calcareous planktonic community (Lisitzin, 1962). Surficial marine sediments to either side of the Polar Front reflect the siliceous or calcareous nature of the planktonic assemblages hosted by the overlying surface water masses.

Thus, Southern Ocean sediments consist of three distinct lithologies, which display a latitudinal zonation (Kemp et al., 1975). Each sediment type forms a belt which circumscribes Antarctica. A zone of glacial pebbly silts and clays lies near the continent and extends across the continental shelf to the abyssal plain. Succeeding this to the north is a belt of siliceous, mostly diatomaceous ooze, which extends laterally to the southern flank of the mid-ocean ridge. The siliceous belt is succeeded to the north by a belt of a foram-nanno ooze (Kemp et al., 1975; Lisitzin, 1971).

The Circum-Antarctic Current is powered by the strong westerly winds of the Southern Ocean region; these winds give the surface water a northeasterly drift and generate the extensive upwelling of deeper, nutrient-laden Circumpolar Deep Water, along the Antarctic Divergence (Gordon, 1971b). The Circumpolar Deep Water replenishes Antarctic Surface Water, which in turn flows in a generally northward

direction to sink in the Polar Front Zone (Figure 1). Consequently, a steady supply of nutrients to the photic zone provides between the Antarctic Divergence and the Polar Front Zone a surface environment with some of the most biologically productive waters in the world's oceans (Lisitzin, 1971). Indeed, the limiting factor to productivity in this province is not nutrients, but light (Edmond, 1975; Burkholder and Burkholder, 1967).

This study is a description and interpretation of the development, location, and intensity of Antarctic productivity during the Cenozoic. Previous studies have related surface productivity in the Equatorial Pacific to calcareous skeletal remains of surface plankton in the sediment (van Andel et al., 1975). However, accumulation of skeletal carbonate is not only a function of carbonate productivity, but also of the position of the lysocline and the calcite compensation depth (Heath and Culberson, 1970), and of the rate of dissolution at depth (Berger, 1970a). Because so many variables affect the preservation of calcium carbonate, it provides only a qualified estimate of surface productivity.

Skeletal opal, in the form of diatom, radiolarian, and silicoflagellate tests, on the other hand, provides a more dependable index for surface productivity (Lisitzin, 1971; Heath, in press). While most of the opaline silica dissolves during its descent through the water column (Wollast, 1974; Hurd, 1974; Lisitzin, 1971), it does not behave like CaCO_3 in that it does not dissolve differentially with depth, and

there exists no "opal compensation depth" (Heath, 1974; Edmond, 1974). However, shallower seafloor sites receive a higher percentage of surface-produced opal than proximal sites which are deeper. This is simply a result of the prolonged exposure to dissolution experienced by skeletal opal en route to deeper regions. This effect must be considered when using opal accumulation to study surface productivity.

Thus, the rate of accumulation of biogenic opal can be used in a better reconstruction of surface productivity than through CaCO_3 accumulation, as demonstrated by Leinen (1976; and in prep), Lisitzin (1971), and Ryther (1963).

Estimates of opal production are a valuable tool to reconstruct past oceanic conditions, because opal productivity is closely associated with upwelling of fertile waters from sub-surface depths. As the location and strength of upwelling varies, so do the location and accumulation rate of biogenic opal in the sediments. Three major factors control mid-ocean upwelling: atmospheric circulation, polar glaciation, and tectonic configuration of land masses. Molina-Cruz (1975; and in press) demonstrated that upwelling in the Equatorial Pacific during the Quaternary was directly related to the position of the prevailing southeast tradewinds. Climatic changes causing shifts in the global wind patterns are reflected in corresponding variations in opal productivity (Pisias, 1976; 1975; Wyrтки, 1974; Hayes and Opdyke, 1967).

Glaciation in the Antarctic affects upwelling south of the Polar Front. During cold periods, increased sea ice production and intensified cooling of surface waters near Antarctica cause more AABW to form, thereby accelerating thermohaline flow and intensifying upwelling near the Antarctic Divergence (Kennett et al., 1974; Johnson, 1972; 1971; Gordon, 1971a; Fletcher, 1969).

Finally, the tectonic evolution of ocean basins can affect upwelling. As the configuration of land masses changes in response to sea floor spreading, uplift, or subsidence, seaways may be created or blocked. As oceanic circulation patterns gradually reorganize, variations in the location and intensity of upwelling may result. For instance, Leinen (1976; and in prep) has suggested that declining opal production in the Central Equatorial Pacific during the Eocene and Oligocene was due to a decrease in the upwelling in the meridional divergence zone resulting from the closure of the Tethys Seaway (Luyendyk et al., 1972) caused by migrating land masses.

Similarly, climatic and tectonic parameters have affected past surface productivity in the Antarctic Ocean which are recorded in the opal content of Antarctic marine sediments.

To study opal variation with time, two D. S. D. P. sites were selected which are located in the Antarctic Ocean between Australia and Antarctica (Figure 2). Combined, these sites contain sediments representing almost the entire Cenozoic period. Site 266 lies at a

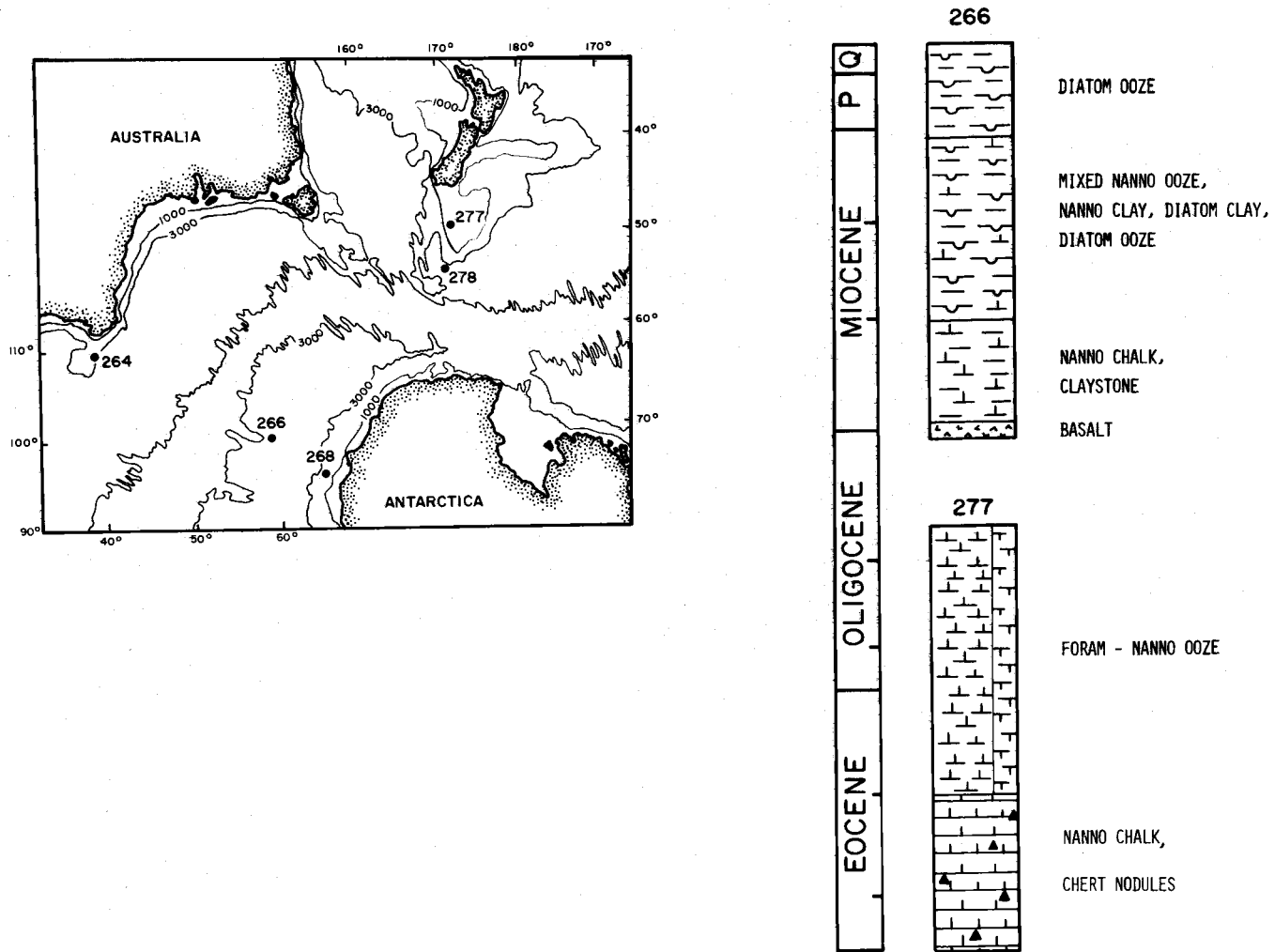


Figure 2. Site location for D. S. D. P. sites used in this study. Biogenic silica accumulation rates were determined for sites 266 and 277. Sedimentary data from site 268 contributed some information to the 5 million-year time gap between sites 266 and 277. Samples were chosen from sites 264, 266, 268, 277, and 278 to study clay-bound silica.

depth of 4167 m, on the southern flank of the Southeast Indian Ocean Ridge, at $56^{\circ} 24.13' S$, and $110^{\circ} 06.70' E$. Its cores consist of 148 m of Quaternary to Late Miocene diatom ooze, grading down to 105 m of mixed nanno ooze, nanno clay, diatom clay, and diatom ooze of Late to Middle Miocene age. This is underlain by 117 m of Early Miocene nanno chalk and claystone, which rest on basement at a depth of 370 m (Hayes, Frakes et al., 1975).

Site 277 is located on the Campbell plateau south of New Zealand, at $52^{\circ} 13.43' S$, $166^{\circ} 11.48' E$, in 1232 m of water (Figure 2). Cores at this site contain 462 m of continuous Eocene and Oligocene nanno oozes, which grade downward into nanno chalks. Silicified chalk layers and chert nodules are found in the Early Oligocene and Eocene chalks. Basement was not reached (Kennett, Houtz et al., 1974).

Based on the opal productivity variations derived from these sites, and using published data on paleoclimatic studies (Savin et al., 1975; Shackleton and Kennett, 1974; Hayes, 1972; Devereaux, 1967, Antarctic circulation and paleocirculation (Hayes, Frakes et al., 1974; Johnson, 1974; 1972; 1971; Gordon, 1972; 1971), sediment studies (Hayes and Frakes, 1975; Kemp et al., 1975; Kennett, Houtz et al., 1975; Jacobs, 1974; Weaver, 1973; and Lisitzin, 1971), and seismic reflection data (Laird et al., 1977; Molnar, 1975; Weissell, 1974; Veevers, 1974; Houtz, 1974; Hayes and Ringis, 1974, and Weissel and Hayes, 1971), the history of the Antarctic biological

productivity can be reconstructed and integrated in a paleoceanographic description of this region during the Cenozoic. This, in turn, leads to further insights into the history of the global thermohaline and surface circulation and in the partitioning of dissolved silica between the Pacific and Antarctic Oceans.

The specific objective of this study is twofold: First, the existing geochemical method for opal determination of marine sediments of any age (Leinen, 1977) is modified in order to apply to the mineralogy of high southern latitude sediments. Leinen (1977) developed a method for opal determination which uses a normative calculation to predict the amount of silica in a bulk sample that is non-biogenic. The remaining silica fraction is considered to be biogenic opal. The equation used to predict non-biogenic opal is derived from Si, Al, and Mg concentrations in Pacific sediment samples. These samples are considered to be representative of the dominant mineralogies encountered in the Pacific region. Thus, the calculation applies specifically to Pacific sediments of high smectite (montmorillonite) content (Leinen, 1977).

In contrast, sediments from the Southern Ocean are dominated by the clay mineral illite, which has a higher Al and lower Mg content than montmorillonite (Cook et al., 1974; 1975; Jacobs, 1974). Because of this, an equation based on Pacific sediment chemistry cannot be used to estimate non-biogenic silica in the Southern Ocean. Instead

a unique equation must be generated from Al and Mg concentrations determined from Southern Ocean sediments.

The second objective of this work is to interpret the variations in opal deposition through time, in terms of the paleoceanographic evolution of the Southern Ocean Basin. In particular, this evolutionary context encompasses:

- (1) the regional tectonism
- (2) the gradual isolation of Antarctica
- (3) the establishing of present surface and thermohaline water mass regimes
- (4) the progressive climatic deterioration
- (5) the initiation of Antarctic glaciation.

A third, but not a primary objective of this study is the comparison of Central Equatorial Pacific opal accumulation rates (Leinen, 1976; and in prep.) to Antarctic opal accumulation rates during Cenozoic times. This comparison is addressed in terms of extrapolated surface production of opal, with implications for the budgeting of silica between the ocean's two most biologically productive upwelling regions.

APPROACH TO OPAL DETERMINATION

To use biogenic silica accumulation rates in paleoceanographic reconstructions, a good estimate of the opal content in each sample is necessary. The reliable determination of opal in sediments is complicated for modern sediments, and was, until very recently, impossible for sediments older than 1 m. y. Techniques used to evaluate opal content include X-ray diffraction (Ellis, 1972; Calvert, 1966; Goldberg, 1958), chemical dissolution and leaching (Kamatani and Oda, 1974; Hashimoto and Jackson, 1960), and infrared spectroscopy (Chester and Elderfield, 1968). A review of these techniques is given by Leinen (1977).

All of these techniques have proven to be unreliable for sediments older than 1 million years. The X-ray diffraction determination of opal, involving the thermal conversion of amorphous opal to crystalline cristobalite, underestimates opal in older sediments because thermal conversion of aged opal to cristobalite is not complete, perhaps because of bond reorganization which alters the molecular structure of opal as it ages (Heath, 1974). A further problem with the X-ray technique is its inability to measure opal which has been dissolved and reprecipitated as a siliceous coating on other sediment grains (Heath, 1974). Bond changes affecting opal structure with increasing age also decrease the solubility of opal (Heath, in

press), and make dissolution techniques for the determination of opal unreliable. Techniques relying on infrared spectroscopy are not accurate for marine sediments with an opal:quartz ratio less than 3; in addition, common marine constituents such as palagonite interfere with the determination (Chester and Elderfield, 1968).

The limitations of these techniques have stimulated subsequent investigators to a reorganization of thinking. Instead of attempting a direct measurement of skeletal opal in pre-Pleistocene sediments, the newest approaches advocate an initial analytical determination of total silica in a bulk sediment, from which quantifiable non-biogenic silica fractions are isolated and subtracted. (Arrhenius (1952) used this approach to biogenic opal determination in the early 1950's.) Quantitatively significant sources of non-biogenic silica in the pelagic realm are detrital quartz and clay-bound silica. When non-biogenic silica phases are subtracted from total silica, the residual is assumed to be biogenic opal, in the relation:

$$\text{BIOGENIC OPAL} = \text{TOTAL SiO}_2 - \text{CLAY-BOUND SILICA} \\ - \text{DETRITAL QUARTZ}$$

The most analytically elusive of the above parameters is clay-bound silica. Leinen (1976; 1977), following the reasoning of Bostrom and Fischer (1971) and Bostrom et al. (1972), proposed to estimate non-biogenic silica in Central Pacific sediments by assuming a constant

$\text{SiO}_2:\text{Al}_2\text{O}_3$ ratio for marine clays. This approach assumes that the opal content of marine sediments of any age can be determined using a normative calculation in which some of the analytical silica concentration is subtracted as non-biogenic, in proportion to the amount of Al or other constituents in the sample. Depending on the age and location of the Pacific samples, Leinen employed one of three $\text{SiO}_2:\text{Al}_2\text{O}_3$ ratios to correct the bulk silica content for non-biogenic silica. For samples 0 to 5 m. y. B. P., a ratio of 3:1 was used. For the other samples, a $\text{SiO}_2:\text{Al}_2\text{O}_3$ ratio of 3.5:1 was used, except for those samples originating near the East Pacific Rise for which a ratio of 4:1 was used.

This approach can be significantly improved with a more detailed normative calculation involving both Al and Mg content of individual samples, which provides for variations in clay mineralogy, and allows for a more versatile utilization of the chemical data (Leinen, 1977). This approach yields reasonable estimates of opal content in pre-Pleistocene sediments as it is unaffected by bond changes which occur in aging opal. In addition, it includes the measurement of opal which has dissolved and reprecipitated onto existing sediment grains.

The method used in this study (Appendix I) involves such a normative calculation, based on the Al and Mg concentrations of bulk sediment. The Al and Mg cations were chosen to characterize the

silica content of clays because of their relationship to each other, and their relation to Si within the clay structure. In a clay mineral, the trioctahedral and dioctahedral site occupations of Al and Mg are related to the site occupation of Si. The amount of Al in the octahedral and tetrahedral sites of the clay mineral structure primarily defines the site space available for Si. Mg is second in importance (Leinen, 1977). Mg substitution for trivalent cations in the octahedral sites of marine clays correlates with the amount of Al substitution for Si in tetrahedral sites. Fe is also an important structural constituent of marine clays, but its relationship to Si and Al is obscured by other sources of iron in sediments; many of these iron phases are amorphous (Leinen, 1977).

Although the cation relationships between Al, Mg, and Si are complex, they can be statistically defined using multiple regression analysis. First, a regression equation defining the relationship between clay-bound Al and Mg, and clay-bound Si is established. Then, this equation can be used to predict clay bound silica from chemical data determined for any Southern Ocean sediment. Once bulk silica values for Southern Ocean sediments are corrected for clay-bound silica, they are further corrected for detrital quartz. The final silica end-member remaining is assumed to be biogenic opal. The accuracy of this technique is about $\pm 5\%$ opal.

ANALYTICAL RESULTS

Results from the laboratory analyses are shown in Figure 3, as % opal, % CaCO_3 , % non-biogenic residue, and % quartz. From these the accumulation rates of the same major constituents have been calculated (Figure 5). Comparing Figures 3 and 5, it is obvious that trends in the accumulation rates are in many cases similar to trends in the concentration curves. To avoid repetition, only a brief summary is devoted to the basic trends in the analytical concentration curves. This is followed by a more detailed discussion of accumulation rates, with particular emphasis on their fluctuations during the Cenozoic.

Opal Content

During the Eocene and Oligocene, opal content on a bulk basis accounts for only 0 to 6% of the opal, displaying a small increase between about 35 and 45 million years before present. A maximum of 6.6% opal at about 40 m. y. B. P. occurs. The carbonate-free opal curve for the Eocene and Oligocene is more varied. A distinct minimum in opal content occurs from about 40 to 50 m. y. B. P. preceded by a maximum content of opal, and followed by another opal peak of equal magnitude. The broad, low-magnitude increase in the bulk opal curve, when considered on a carbonate-free basis, resolves into a series of maxima and minima, which are superimposed onto a

broad peak spanning from about 32 to 48 m. y. B. P.

Average biogenic silica content at site 277 during the Eocene and Early Oligocene may be slightly higher than the values measured in this study. This is because of chert nodules and regions of silicified chalk, which both occur in the Eocene and Oligocene nannofossil chalks at site 277. In analyzing the sediments at site 277, samples were chosen which were characteristic of the dominant lithology. The frequency of occurrence is about 1 chert nodule or silicified region per 10 meters of core. The nodules are a few centimeters in diameter (Kennett, Houtz et al., 1974). Because chertified sediments were not truly representative of the bulk sediment, samples containing them were not chosen for analysis.

From the Neogene to the present the decreasing carbonate content causes the corresponding bulk and carbonate-free opal curves to be very similar. The bulk opal curve trends from a high of 16% opal 23 m. y. B. P. to negligible opal content from about 13 to 19 m. y. B. P. Subsequently, the opal content goes through a double-lobed peak from about 8 to 13 m. y. B. P. Thereafter, a rapid increase begins, which contains a single-point minimum at about 6 to 8 m. y. B. P., followed by a dramatic increase which climbs to the present all-time maximum opal content of 70%.

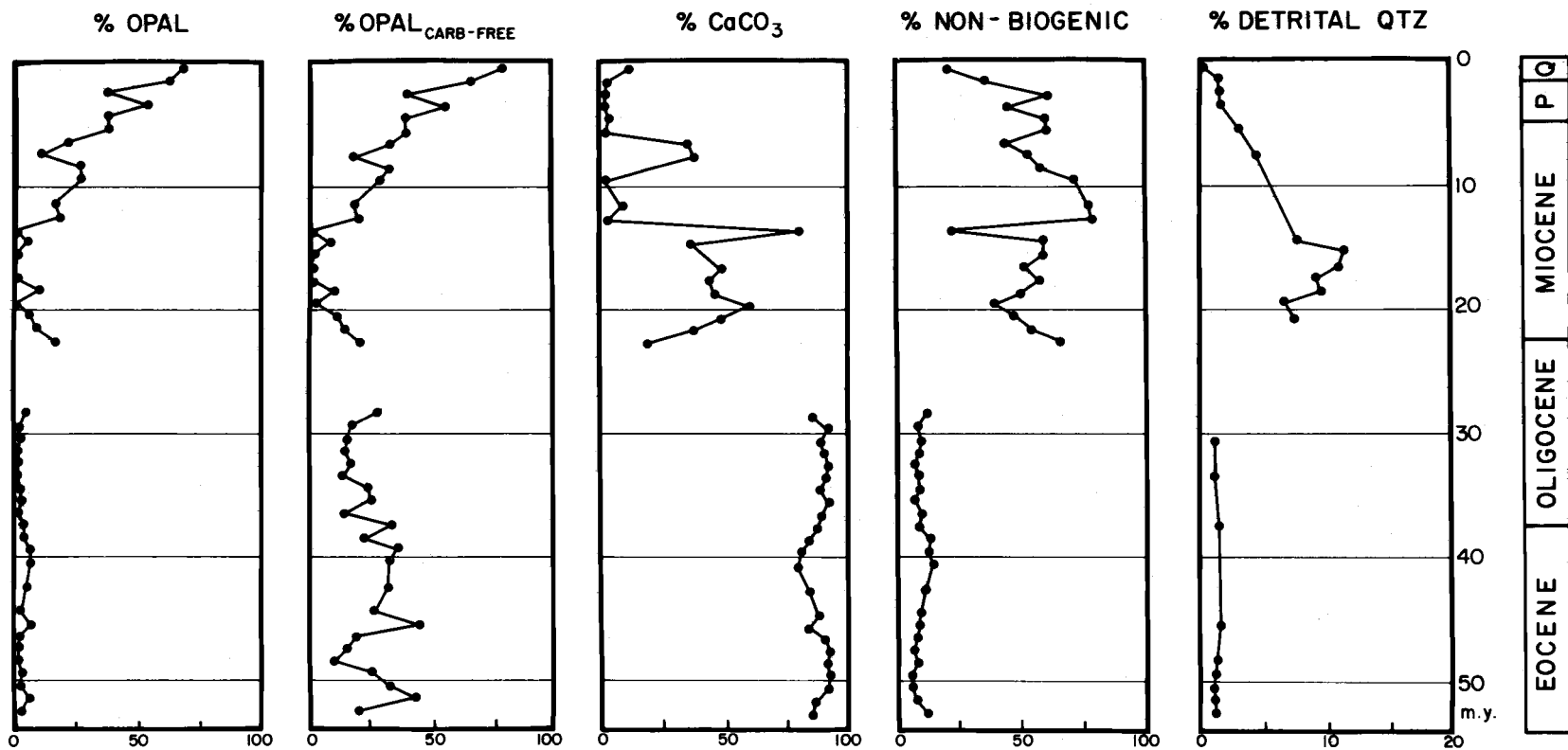


Figure 3. Analytical salt-free concentrations of sedimentary components at sites 266 and 277. All components except % opal (carbonate-free) are presented on a bulk sediment basis. % Non-biogenic content is determined by subtracting % opal + % CaCO₃ from 100%.

Calcium Carbonate Content

A plot of calcium carbonate content from sites 266 and 277 systematically displays trends which are opposite to trends in opal content. During Eocene and Oligocene times, site 277 was an area of pelagic clacareous sedimentation (Kennett et al. , 1974); this is reflected in the stable high values (between 80 and 92% CaCO_3) at site 277 (Figure 3). A broad decrease extends from about 35 to 45 m. y. B. P. , reaching a minimum about 40 m. y. B. P. of 79% CaCO_3 .

The Neogene to present curve, like the opal curve, displays more interesting variations, with peaks at 20 m. y. B. P. , 13 m. y. B. P., and from 6 to 8 m. y. B. P. Lows occur at 23 m. y. B. P. and from 14 to 19 m. y. B. P. The most recent low occurs from 2 to 5 m. y. B. P. , when CaCO_3 accounted for only 2% of the total sediment.

Calcium carbonate concentration began to increase again about 1 m. y. B. P. , to 11% CaCO_3 at present.

Non-Biogenic Residue Content

The non-biogenic residue content was calculated by subtracting the sum of opal content and CaCO_3 content from 100%. The components of this fraction are dominantly clay, with varying minor amounts of terrigenous detritus and amorphous ferromanganese oxides. Because the sediments at site 277 all contain nearly 90% calcium

carbonate and opal content is minimal, the non-biogenic curve for the corresponding time interval is the inverse of the CaCO_3 curve (Figure 3). This relationship continues through to the Late Miocene (about 8 m. y. B. P.) of site 266, at which time siliceous sedimentation begins to dominate and the non-biogenic curve becomes instead a mirror image of the opal curve. Subtracting % quartz from % non-biogenic content yields a rough estimate of clay content in the samples. These values are plotted vs. time in Figure 4. Corresponding values of % Al and % Mg determined from atomic absorption spectroscopy are also shown. Also shown is the clay-bound silica curve. The agreement of these curves is (and must be) very close in order to confirm that in Southern Ocean sediments there are no significant sources of Al or Mg other than clay. An example of an extraneous source of Al might be volcanic glass. This provides further confidence in the clay-bound silica values, which were predicted from Al and Mg concentrations.

Detrital Quartz Content

A portion of the non-biogenic content consists of detrital quartz, presumably deposited from ice originating on the Antarctic continent (Kennett et al. , 1974); Quartz accounts for between 1 and 2% of the bulk sediment at site 277, but is higher at site 266 (about 9 to 10%), in the Early and Middle Miocene. Quartz reaches a maximum of

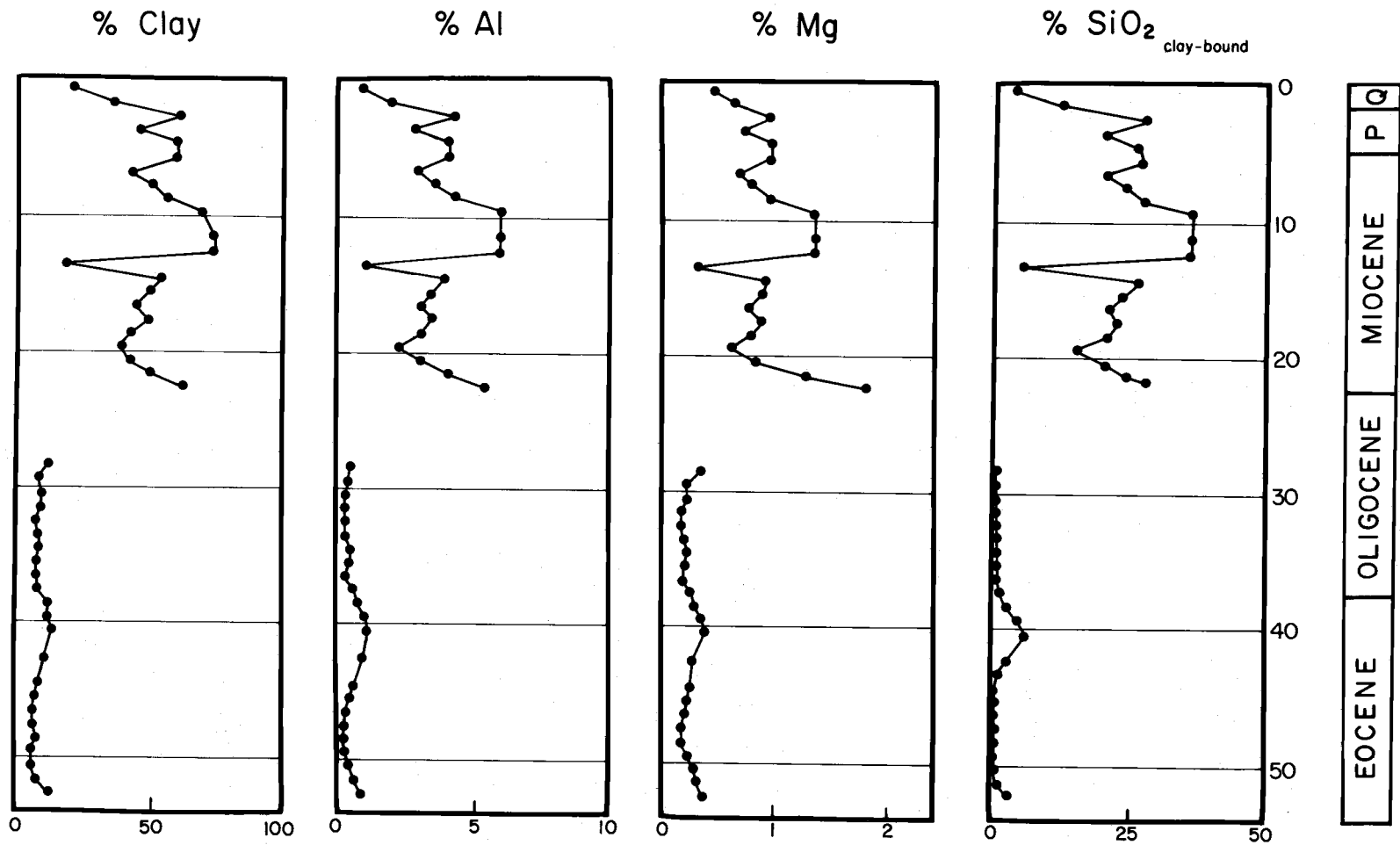


Figure 4. Analytical concentrations of Al and Mg, corrected for salt and presented on a bulk sediment basis. % Clay is determined by subtracting % quartz from % non-biogenic content, and as such, as an estimation. % Si (clay-bound) is predicted from Al and Mg concentrations according to the regression equation. The good agreement of the first three curves confirms the fact that there are no significant sources of Al and Mg except for clay.

10.6% at about 15 m. y. B. P. Thereafter the detrital quartz content decreases to the present minimum.

Accumulation Rates

Cenozoic sedimentation rates, bulk sediment accumulation rates, and accumulation rates for opal, CaCO_3 , and non-biogenic fractions are displayed in Figure 5. Sedimentation rates were taken from the sediment age vs. depth in hole curves in the D. S. D. P. site reports for sites 266 and 277 (Hayes, Frakes et al., 1975; Kennett, Houtz et al., 1974). Using GRAPE data from computer plots provided by the D. S. D. P., bulk densities (ρ) and porosities (ϕ) were used in calculating bulk accumulation rates according to the relation:

$$\text{bulk accumulation rate} = 100 (\rho - 1.025\phi) \text{ sed. rate}$$

after van Andel et al. (1975), which includes a salt correction. Multiplying % component (e. g. % opal) by bulk accumulation rates provides accumulation rates for each component (Appendix IV). Considering sedimentary constituents on an accumulation rate basis frees the constituents from the effects of dilution and compaction (van Andel et al., 1975), and introduces a time factor into the values.

Site 266 extends from the present to 23 million years before present, site 277 from 28 to 53 m. y. B. P. Combining these two sites yields an almost complete Cenozoic time sequence, except for the

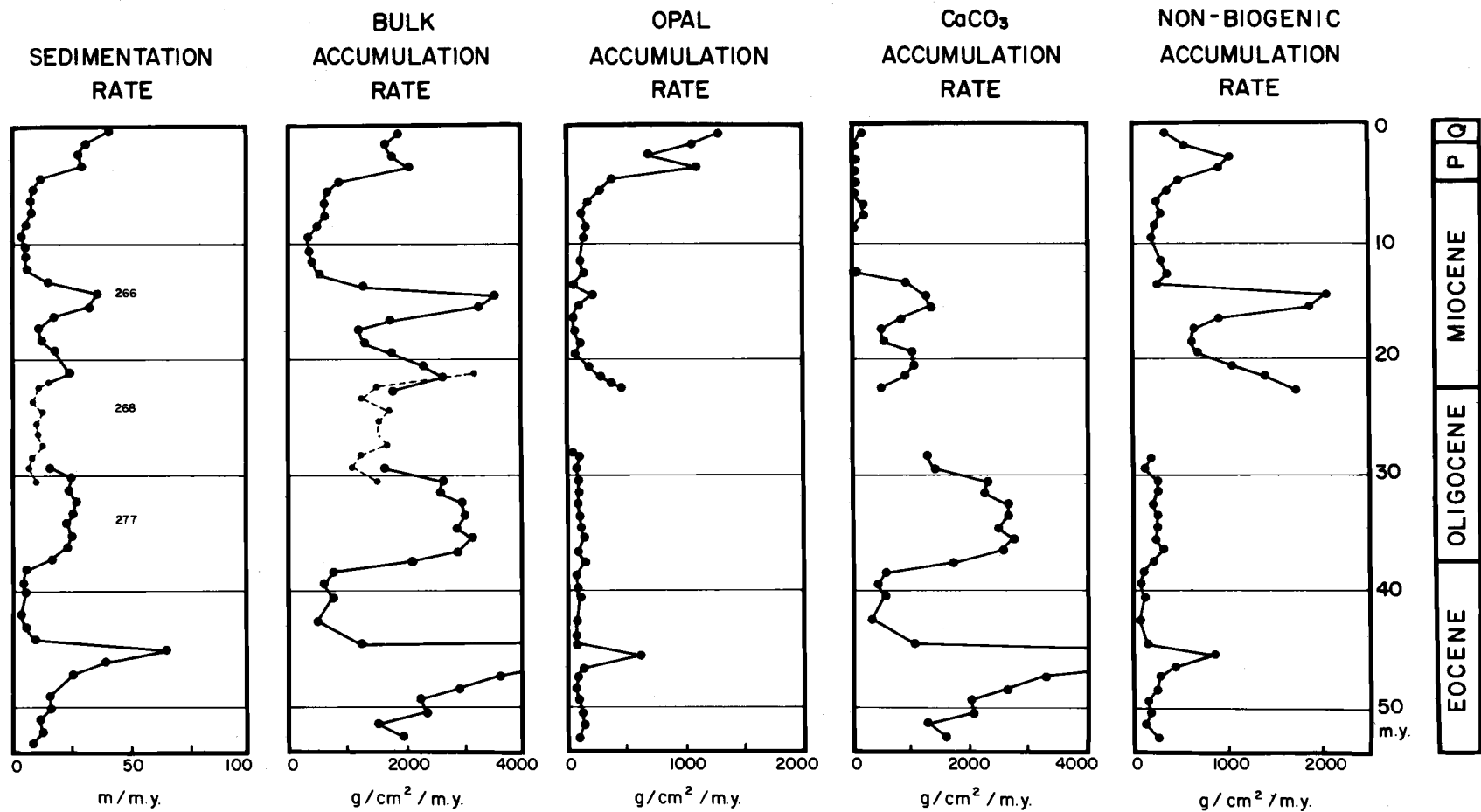


Figure 5. Sedimentation rates and accumulation rates of bulk sediment, and sedimentary components at sites 266 and 277; dashed curves are from site 268. All components are corrected for salt, and calculated on a bulk sediment basis. The Middle Eocene peak in sedimentation rate is based on poor biostratigraphic information, and is probably too high.

Paleocene and a 5 million year gap from 23 to 28 m. y. B. P. To make the data base more complete, information from nearby site 268 was used to gain some knowledge of sedimentation during the Late Oligocene-Early Miocene time gap. Assuming that it adequately represents the general trend in sedimentation for the region, sedimentary data from site 268 indicate relatively low and constant rates of sedimentation prior to 24 m. y. B. P. (about 10 m/m. y.), increasing to a high of 25 m/m. y. 22 m. y. B. P. , at which time the sedimentation rates for 266 and 268 are the same. If this increase of the sedimentation rate in the Early Miocene is accepted as characteristic of the region it can be used to fill the gap from 23 to 28 m. y. B. P. The corresponding bulk accumulation rates for 268 are used to fill in the gap in the bulk accumulation rate curve.

In the sedimentation rate and bulk accumulation rate curves, five peaks are evident during the Cenozoic at 0 to 5 (40 m/m. y.), 13 to 16 (37 m/m. y.), 22 (23 m/m. y.), 30 to 36 (26 m/m. y.), and 45 to 47 m. y. B. P. (67 m/m. y.). The recent sedimentation rate of 40 m/m. y. is consistent with the sedimentation rate determined by Kharkar et al. (1969), of 47.2 m/m. y. , based on ^{32}Si . The 45-47 m. y. peak is unreasonably high, probably because of very poor stratigraphic control in that portion of the core (Kennett, Houtz et al. , 1974), and has produced similarly high peaks in the accumulation rate curves.

Maximum values in bulk sediment accumulation associated with the maxima of these same five peaks in sedimentation rate are: 1800 g/cm²/m. y. (for 0 to 5 m. y. B. P.); 3500 g/cm²/m. y. (for 13 to 16 m. y. B. P.); 2600 g/cm²/m. y. (for 22 m. y. B. P.); 3100 g/cm²/m. y. (for 30 to 36 m. y. B. P.); and an unreasonably high 8800 g/cm²/m. y. (for 45 to 47 m. y. B. P.).

Times of low sedimentation and consequent low accumulation are from about 5 to 12 (3.5 m/m. y.), 16 to 20 (11 m/m. y.), 23 to 28 (8 m/m. y.) (inferred from site 268), 37 to 43 (3 m/m. y.), and immediately prior to 48 m. y. B. P. (9 m/m. y.). The low bulk accumulation rates corresponding to these minima are, respectively: 400 g/cm²/m. y. (for 5 to 12 m. y. B. P.); 1140 g/cm²/m. y. (for 16 to 20 m. y. B. P.); 1025 g/cm²/m. y. (inferred from site 268 for 23 to 28 m. y. B. P.); 390 g/cm²/m. y. (for 37 to 43 m. y. B. P.); and, finally, 1480 g/cm²/m. y. (for prior to 48 m. y. B. P.).

It is interesting to note that fluctuations in Antarctic sedimentation and bulk accumulation rates correspond very closely to sedimentation and accumulation rate trends in the Pacific (see Figures 5 and 6). In both Pacific and Antarctic data sets the periods of high sedimentation and accumulation are of shorter duration, and times of low sedimentation are more prolonged. In particular, the times of low carbonate accumulation are essentially simultaneous.

The opal accumulation rate curve resembles a smoothed version

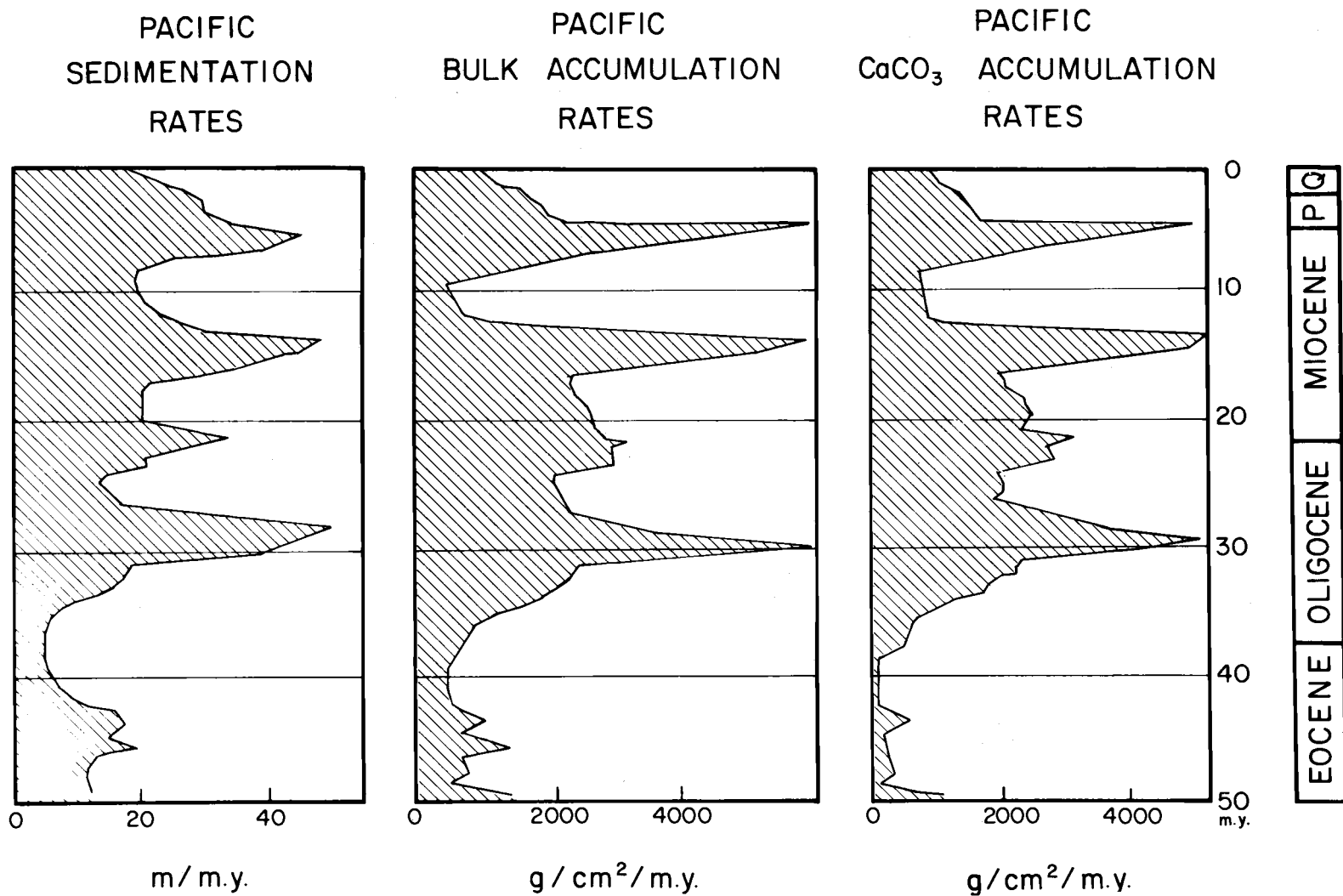


Figure 6. Generalized Cenozoic Pacific sedimentation rates and accumulation rates for both bulk sediment and CaCO₃. Generalized curve trends taken from van Andel et al., 1975.

of the opal content curve. Eocene and Oligocene times are characterized by low, constant accumulation of opal, at an average rate of $40 \text{ g/cm}^2/\text{m. y.}$, except for the peak at 46 m. y. B. P., which is, as discussed, too high. However, this peak is not entirely an artifact of high sedimentation rates; a slight increase in opal content to 6.6% occurs at this time as well.

Between 23 and 28 m. y. B. P. opal accumulation rates are not known. However, fairly high accumulation rates are indicated at the beginning of the Miocene, with an opal accumulation rate of $412 \text{ g/cm}^2/\text{m. y.}$, except for the peak at 46 m. y. B. P., which is, as discussed, too high. However, this peak is not entirely an artifact of high sedimentation rates; a slight increase in opal content to 6.6% occurs at this time as well.

Between 23 and 28 m. y. B. P. opal accumulation rates are not known. However, fairly high accumulation rates are indicated at the beginning of the Miocene, with an opal accumulation rate of $412 \text{ g/cm}^2/\text{m. y.}$. Thereafter, opal accumulation decreases until about 8 m. y. B. P., passing through a period of negligible opal accumulation at 13 m. y. B. P. and again from 16 to 18 m. y. B. P. Otherwise, rates remain fairly constant near $100 \text{ g/cm}^2/\text{m. y.}$. One minor increase occurs about 14 m. y. B. P. which is attributed to an increase both in opal content and in sedimentation rate. From 8 m. y. B. P. to 5 m. y. B. P. opal accumulation begins to accelerate. An initial rapid fourfold

increase in opal accumulation rates to $1100 \text{ g/cm}^2/\text{m. y.}$ at about 5 m. y. B. P. is followed by a temporary decrease to $666 \text{ g/cm}^2/\text{m. y.}$ about 3 m. y. B. P. From 3 m. y. B. P. to present opal accumulation rates have increased to the present Cenozoic maximum of $1240 \text{ g/cm}^2/\text{m. y.}$

The carbonate accumulation rate curve for Eocene and Oligocene times essentially duplicates the corresponding curve of bulk sediment accumulation as is to be expected from the high calcium carbonate content of the sediment. Moderate to high Eocene rates are followed by a Late Eocene to Earliest Oligocene low of $325 \text{ g/cm}^2/\text{m. y.}$, which is succeeded by a broad peak from 30 to 36 m. y. B. P. (to $2770 \text{ g/cm}^2/\text{m. y.}$). Carbonate accumulation decreases in the Miocene with small variation. From 13 m. y. B. P. to the present, calcareous sedimentation has played a minor role at site 266, with rates near $30 \text{ g/cm}^2/\text{m. y.}$

The non-biogenic accumulation rate curve for the Eocene and Oligocene is very similar to the curve displaying opal accumulation, i. e., low constant values of about $100 \text{ to } 200 \text{ g/cm}^2/\text{m. y.}$, with a (probably erroneous) peak at 46 m. y. B. P.

Accumulation of non-biogenic material in the Miocene is characterized by a peak of $1700 \text{ g/cm}^2/\text{m. y.}$ (22 m. y. B. P.), followed by a low of $600 \text{ g/cm}^2/\text{m. y.}$ (7 to 19 m. y. B. P.). A short-lived but high magnitude increase of $2000 \text{ g/cm}^2/\text{m. y.}$ in non-biogenic accumulation

occurs in the Middle Miocene, about 14 to 16 m. y. B. P. This increase is succeeded by a second period of low, constant accumulation rates, from 6 to 13 m. y. B. P. (200 to $360 \text{ g/cm}^2/\text{m. y.}$). A final peak in non-biogenic residue occurs from 2 to 5 m. y. B. P., reaching a high value of $100 \text{ g/cm}^2/\text{m. y.}$ Thereafter non-biogenic sedimentary components decrease in importance.

Dissolution of Opal and the Opal Supply to Bottom Sediments

Opal accumulation rates have been used to infer surface productivity. In order to justify an estimate of surface production of opal, the effect of dissolution must first be evaluated.

Seawater is undersaturated with respect to amorphous silica (Johnson, 1975; Schink et al., 1974; Siever and Woodford, 1973; Heath and Dymond, 1973). While the equilibrium solubility for opal is $1030 \mu\text{M}$ at 2°C and 500 b (Jones and Pytcowicz, 1973), normal seawater ranges from as low as $0 \mu\text{M}$ in surface waters to $180 \mu\text{M}$ in deeper waters (Heath, in press). Nowhere in the open ocean is seawater saturated with respect to opaline silica. Of the silica fixed biologically in the surface waters, only a small percentage survives to become permanently incorporated into the bottom sediments, while the bulk is dissolved as the skeletons descend through the water column (Heath, 1974; Calvert, 1968; Hurd, 1974; Johnson, 1975). Approximations of siliceous surface plankton populations based on

carbon-14 measurements (Koblentz-Mishke et al., 1970; Lisitzin, 1967), when compared to opal content of underlying surface sediments, indicate that about 97% (Wollast, 1974) to 98% (Heath, 1974; Lisitzin, 1971) of the opal dissolves during its descent. The dissolved silica is recycled to the photic zone, via upwelling or eddy diffusion generated by concentration gradients between deeper waters, enriched in silica, and silica-stripped surface waters (Wollast, 1974).

The fate of the 2-3% opal which escapes dissolution in the water column is less certain. Some opaline tests at the sediment/water interface dissolve before burial. Interstitial pore waters contain higher concentrations of dissolved silica than seawater (from 315 μM in Atlantic sediments, to 999 μM in Pacific siliceous oozes, Heath, in press), indicating that further dissolution of opal takes place in the sediment column. Dissolved silica concentrations increase downward. The concentration gradient suggests that some process is active in removing silica from the upper few centimeters of the sediment. A minor portion of the dissolved interstitial silica presumably diffuses out of the upper few centimeters due to concentration gradients between the bottom water and the pore water. However, experimental work by Johnson (1975) has shown that the amount of silica diffusing into the ocean from the sediment estimated in previous studies (Wollast, 1974; Schink et al., 1974; Heath, 1974; Hurd, 1973) is too high.

Bioturbation in the upper 15 cm of sediment resuspends opal, thereby exposing it to further attack by dissolution. In addition, bioturbation advects some silica which has already dissolved interstitially (Johnson, 1975).

Processes which permit the persistence of skeletal opal deeper in the sediment column despite silica-undersaturated pore waters are more complex. Lewin (1961) suggested that metal cations such as Al, Mg, and Fe are adsorbed onto the walls of opaline skeletons, possibly to such an extent that simple aluminosilicates are formed on the test (Hurd, 1974). The cations retard dissolution of opal, and may enable the opal to remain intact in a metastable equilibrium.

More important, a complex equilibrium may be generated by clay silicate--opal interactions (MacKenzie and Garrells, 1966; Sillen, 1961). In clay-rich sediments of low opal content, opal may continue to dissolve interstitially to be incorporated into clay minerals until all the opal has dissolved and been assimilated. In sediments with abundant opal and some clay, an opal--clay equilibrium below the equilibrium saturation for opal may be established after the clays have consumed dissolved silica to their capacity (Suess, in prep).

Where abundant iron is present, as in the Bauer Deep, or near mid-ocean ridges, dissolved opal may react interstitially with iron and compatible elements to form an authigenic iron-rich smectite (Heath and Dymond, in press).

The minute fraction of skeletal opal fortunate enough to avoid post-burial dissolution and chemical fixation is retained in the geologic record. Wollast (1974) is somewhat ambiguous in his estimation of this fraction. His silica budget, based on mass balance of silica, yields a mean opal preservation factor of .3% opal preserved, but his opal concentration in sediments vs. silica input from rivers suggests the amount preserved to be .6%, or 20% of the estimated 3% reaching the seafloor. For the Antarctic, both of Wollast's preservation factors yield excessively high values for surface production of opal, based on analytical opal measurements from this study. A more reasonable approximation of opal preservation with specific respect to Southern Ocean sediments is 1% opal. This percentage yields a value for surface productivity of $1240 \text{ g opal/m}^2/\text{yr}$ for the last m. y., which is more consistent with Lisitzin's (1971) rough estimate of present productivity of "greater than $500 \text{ g opal m}^2/\text{yr}$." Thus, a post-burial opal preservation factor of .3% apparently does not apply to the Southern Ocean sediments, for two reasons. First, some parameters unique to the Antarctic region may enhance post-burial preservation of opal. Support for this theory exists:

- (1) Diatoms, radiolaria, and silicoflagellates from the Southern Ocean are very well preserved (Chen, 1975; Cielieleski, 1975; Weaver, 1973; Lisitzin, 1971), suggesting little post-mortem dissolution of more robust forms.

- (2) Fertile Antarctic surface waters support prolific higher-order production that contributes to the sediment a greater percentage of fecal pellets. This organic fecal material rapidly transports opal to the seafloor without appreciable dissolution (Schrader, 1971).
- (3) Relatively high Antarctic sedimentation rates from combined terrigenous and biogenous sources rapidly bury and isolate opal from silica-undersaturated bottom waters.
- (4) Silica-depleted clays such as kaolinite, which are abundant in equatorial regions are minor constituents of Antarctic sediments, and can therefore not be responsible for significant uptake of silica. Any silicate--opal reactions involving uptake of silica in the Antarctic are confined to such clays as illite and montmorillonite, which have a lower capacity for silica uptake.
- (5) High concentrations of elements conducive to formation of authigenic smectites, such as Fe, Cu, and Zn, found in the metalliferous sediments of the Bauer Deep (Heath and Dymond, in press), are not as abundant in Antarctic sediments as in the Bauer Deep (Hayes, Frakes et al., 1975), and authigenic smectite formation is probably minimal.

On the whole, the best evidence for increased Antarctic opal preservation is the general agreement of the extrapolated and observed

opal production, assuming 1% preservation instead of 0.3%.

Second, values used in the determination of Wollast's silica budget are values averaged over the world's oceans, and as such are not intended for application in specific oceanic situations. For example, Wollast bases his percent of long-term opal preserved on an average % surface sediment opal to % post-burial opal ratio. He estimates an average opal content of surface sediments to be 8.9%, and an average downcore opal content of 1.9%. Both of these average opal concentrations are too low when compared to analytical concentrations determined for Antarctic sediments in this study. Furthermore, the value of 8.9% for surface sediment opal is probably too low even when considered as an average value. This is due to the limits of our present seagoing technology, which prohibit the recovery of a sediment surface sample without some loss of unconsolidated surface opal. What most workers use as a surface sediment sample, more likely comes from several centimeters below the actual surface, at a depth where considerable opal dissolution has already occurred.

Thus, it is not advantageous to apply a generalized silica model to any specific area, as these models are based only on mass balance of rough estimates of silica input from various sources in the literature.

A revised model depicting the silica budget for the Antarctic Ocean is presented in Figure 7. The 1% opal preservation factor has

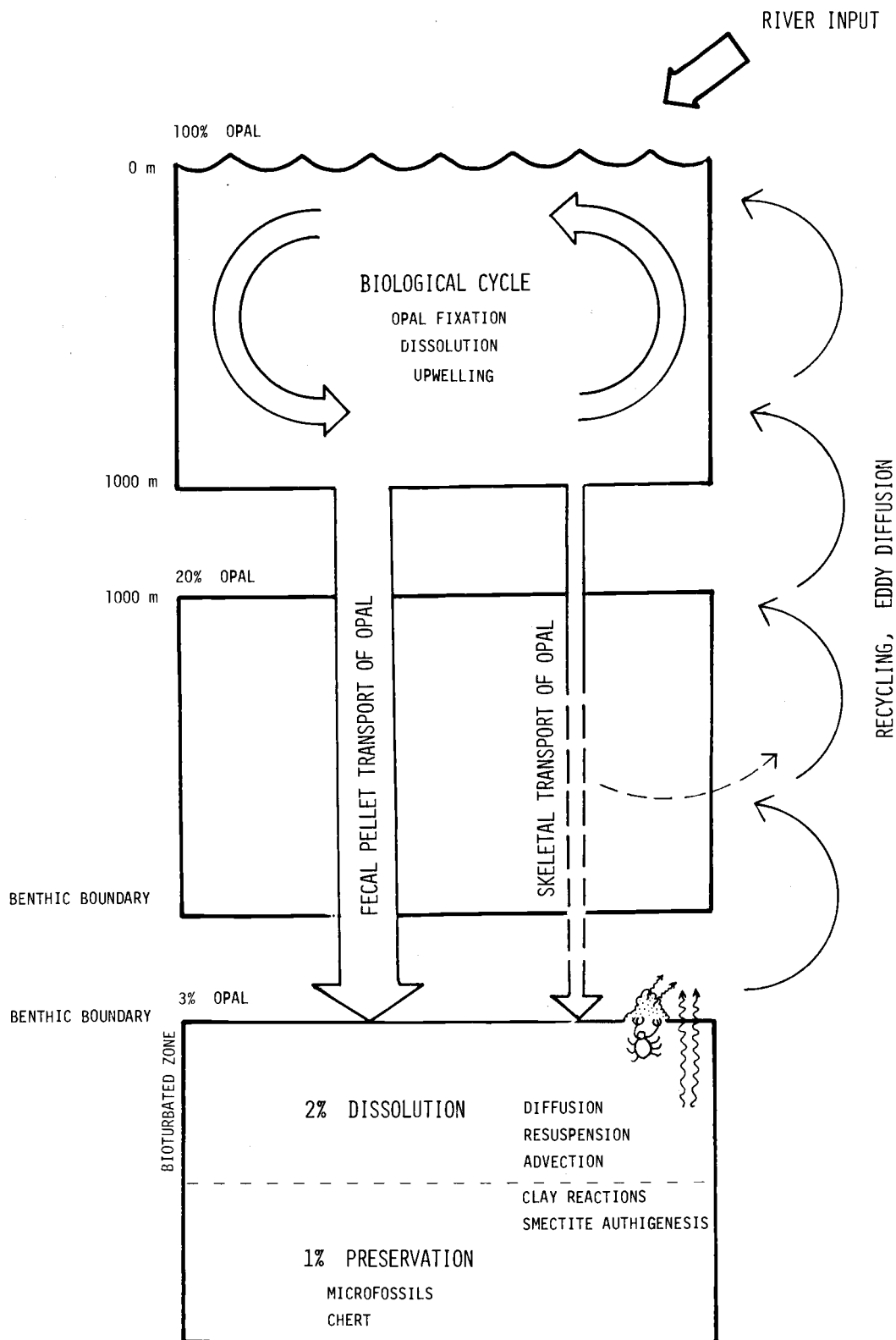


Figure 7. Silica cycle in the Antarctic Ocean. All percentages are in terms of initial input of opal produced in the surface waters.

been used to estimate past surface productivity of opal.

For the purpose of this study, it is assumed that the degree of Antarctic opal dissolution, both in the water column, and in the marine sediments, has not varied significantly during the Cenozoic. At present, no quantitative dissolution studies can test the validity of this assumption, although it is not unreasonable to suggest that some variations in opal dissolution may have occurred. Any long-term changes in the nature of opal dissolution would most likely occur in the upper 1000 meters of the ocean, within the biological cycle (Figure 7). It is in this region where the majority of the opal fixation and dissolution occurs. The residence time of skeletal opal in the biological cycle depends partially on the settling rate of both the free floating and fecal pellet-encased skeletons. More important is the rate of degeneration of the skeletal organic covering (whether it be part of the organism's original organic tissue or fecal pellet material). If degeneration is rapid, the skeleton dissolves while within the biological cycle. Conversely, a slow decomposition of the coating will inhibit dissolution and may allow the skeleton to escape the biological cycle, and may give the opal a greater chance to reach the sea floor. Any long-term variation in the dissolution of opal may well involve the chemical processes active in the biological cycle. Changes in these chemical processes may particularly effect the rate of decomposition of the skeletal organic coating, and thereby moderate

opal dissolution.

The effects of seafloor subsidence and gradual deepening of the Southern Ocean basin on the amount of surface-produced opal reaching the sea floor are considered to be negligible.

TECTONIC, GLACIAL, AND PALEOCEANOGRAPHIC HISTORY OF THE SOUTHERN OCEAN

In order to establish a historical context for the discussion of the history of surface productivity, a summary is presented here after Kennett (in press), which outlines the evolution of the Antarctic's tectonic, glacial, climatic, and circulatory events which may have effected Cenozoic surface productivity.

The Antarctic continent has remained in a high latitude position at least since Mesozoic times (Lowrie and Hayes, 1975). About 80 m. y. B. P., New Zealand broke away from Gondwanaland and began spreading at a rate of 9 cm/yr (Molnar et al., 1975), along a now-buried ridge, thus forming the Tasman Sea (Hayes and Ringis, 1973). Spreading continued until 55 m. y. B. P. when it ceased entirely. During the Eocene, the southern Tasman Sea (and site 277) experienced restricted calcareous pelagic sedimentation (Kennett, Houtz et al., 1974). The Antarctic climate at this time was cool and temperate, and Antarctica was largely non-glaciated (Kemp and Barrett, 1975; McIntyre and Wilson, 1966; Cramwell et al., 1960).

About 55 m. y. B. P., the direction of relative plate motion in the South Pacific changed, and Australia began to rift from Antarctica. Spreading began along the Pacific-Antarctic Ridge at the rate of about 4 cm/yr (Molnar et al., 1975). In the Early Eocene, Antarctic climate began to cool and in general, the temperature continued to

decrease throughout the Cenozoic (Shackleton and Kennett, 1974). Sluggish circulation characterized the evolving ocean basin (Andrews et al., 1975), because circumpolar flow was still blocked by the continental South Tasman Rise, and the southern tip of South America, both still attached to Antarctica (Kennett, Houtz et al., 1974). By about 40 m. y. B. P., Australia had drifted about 1000 km north of Antarctica (Weissel and Hayes, 1972); the South Tasman Rise had begun to submerge, and permitted shallow circulation to connect the South Pacific and South Indian Oceans (Kennett, Houtz et al., 1974). As Antarctica became increasingly isolated, climate continued to cool. Marine sedimentation adjacent to the continent during the Late Eocene consisted of calcareous deposits; siliceous sedimentation was minimal but increasing in importance (Kemp et al., 1974).

Near the Eocene/Oligocene boundary, about 38 m. y. B. P., oceanic surface and bottom temperatures dropped dramatically (Shackleton and Kennett, 1974; Savin et al., 1975). This rapid cooling represents the first major Cenozoic glaciation on Antarctica. Although no ice caps developed, extensive sea ice formed around the Antarctic continent, producing AABW, thereby generating thermohaline circulation that may have been somewhat similar to that of the present ocean (Kennett, in press).

By the Early Oligocene, planktonic and benthic foraminiferal assemblages had adopted their present cold-water characteristics of

low diversity, and simple morphology (Kaneps, 1975). The accelerated northward flow of AABW during the Early Oligocene was responsible for widespread deep-sea erosion (Kennett, Houtz et al., 1974; Kennett et al., 1972).

By the Middle to Late Oligocene, the South Tasman Rise cleared Victoria Land, Antarctica (Kennett, Houtz et al., 1974) and the Drake passage began to open (Barker and Burrell, 1976), permitting circumpolar flow around Antarctica sometime between 25 and 30 m. y. B. P. This caused major reorganization of circulation and sedimentation patterns in the Southern Ocean. The deep-seated Circum-Antarctic Current began to erode bottom sediments south of Tasmania. The belt of siliceous sedimentation expanded, displacing calcareous deposits northward. Bottom water activity in the northern Tasman Sea diminished and was redirected to form a deep western boundary current flow east of New Zealand (Kennett, in press). These deep sea circulation patterns established in the Late Oligocene have persisted to the present, although the overall intensity of circulation has fluctuated.

By the Early Miocene, the Antarctic Surface Water mass with siliceous plankton and cold temperatures can be distinguished from the cool Subantarctic Surface Water with a dominantly calcareous plankton. Oceanic turnover accelerated, and upwelling, although sluggish, was present. Sedimentation rates began to increase,

marking the development of the Polar Front Zone. The influence of the Antarctic Surface Water continued to expand and push the siliceous/calcareous sediment boundary northward (Hayes and Frakes, 1975).

In the Middle Miocene, about 14 m. y. B. P., the temperature dropped, marking a major Antarctic glacial epoch which generated the East Antarctic ice cap (Shackleton and Kennett, 1974). The ice cap has since experienced fluctuations in volume, but has persisted as a permanent feature of Antarctica (Savin et al., 1975).

A major expansion of the ice cap about 5 m. y. B. P. caused a rapid northward shift of the Polar Front of about 300 km, with an associated northward advance of the siliceous belt of sedimentation. Sea level dropped eustatically in response to the formation of extensive sea and shelf ice (Kennett, in press). Continued global cooling produced the glaciation in southern South America about 3.5 m. y. B. P. The Northern Hemisphere became glaciated 2.5 to 3 m. y. B. P., and has since oscillated between glacial and interglacial periods (Shackleton and Kennett, 1974). Progressive cooling in the Quaternary was accompanied by accelerated surface and thermohaline circulation in the Southern Ocean.

DISCUSSION

Surface Productivity and Sedimentation in the Antarctic Ocean: Eocene and Oligocene

From the Eocene through the Middle Oligocene surface productivity was fairly low, confined almost entirely to nanoplankton. This is to be expected as the temperate ocean basin experienced only restricted sluggish circulation with no upwelling (Kennett, in press). Because opal production remains constant, the low CaCO_3 accumulation rates in the Late Eocene cannot indicate a decrease in surface productivity. Instead, the calcium carbonate decrease results from a shallow Late Eocene CCD in the Southern Ocean, similar to the shallow Late Eocene CCD in the Pacific, Atlantic, and Indian Oceans (van Andel, 1975; van Andel et al., in press; Sclater et al., in press).

The cause of the abrupt cooling in the Southern Ocean about 38 m. y. B. P. is not known. Cooling may have resulted from the thermal isolation of the Southern Ocean caused by the closure of the Tethys seaway. The Tethys current presumably circulated east to west from the Atlantic, through to the Pacific, via the passage between North and South America, across the Pacific to the Indian Ocean. This current may have carried warmer waters southward into the Indian Ocean, into contact with polar waters, and caused a thermal latitudinal mixing of waters from all major oceans. As land

masses were tectonically rearranged, the Tethys current was increasingly inhibited until finally, about 38 m. y. B. P., the seaway was closed (Moberly, 1972; Luyendyk et al., 1972). With diminished equatorial current flow, mixing would decrease, circumpolar surface temperatures would drop and sea ice might form. As yet, no other event that might be related to the drop in temperature is known to have occurred at this time. A slight increase in non-biogenic accumulation during the Early and Middle Oligocene indicates some concurrent contribution to sediment accumulation by ice-rafted detritus.

Simultaneously, productivity increased slightly. Sedimentation rates also increased. This is partially due to a rapid lowering of the CCD, which permitted the increased preservation, hence accumulation, of calcareous components. Preservation might also be enhanced by some initial production of AABW, which may have carried away stagnant bottom waters of high CO_2 content (Berger, 1970b; van Andel et al., 1975). The abrupt drop in CCD was apparent throughout the world's oceans (van Andel, 1975; van Andel et al., in press; Sclater et al., in press).

A decrease in accumulation rates of all components about 31 m. y. B. P. and a subsequent period of low sedimentation is most likely due to the reorganization of circulation and sedimentation patterns following the opening of the circumpolar seaway in the Late Oligocene. Sediments which had previously settled in partly isolated Antarctic

basins of sluggish circulation were now swept into a current circling Antarctica. This resulted in a largely non-depositional sediment regime, evidence by Late Oligocene unconformities, as sediments underwent a massive eastward redistribution (Kennett, in press). A considerable portion of this predominantly calcareous material most likely experienced dissolution.

The nature of biogenic productivity during the 5 million year time gap is not known. However, sediments during this time from nearby site 268 consist of chertified clay, suggesting considerable opal production and ice rafting (Kennett, Houtz et al., 1974). Surface productivity at the beginning of the Miocene was quite high, suggesting that sometime between 24 and 28 m. y. B. F. surface production began to increase.

Surface Productivity and Neogene Paleotemperatures

Surface productivity in the Neogene varied considerably, compared with the fairly constant low level of productivity during the Paleogene. Variations in climate, surface circulation, and upwelling caused the Neogene departure from constant productivity. Each of these parameters had an increasing effect on productivity as the Southern Ocean basin expanded, and Antarctica became more and more isolated. The parameter which has had the greatest effect on Neogene surface productivity appears to be temperature. Figure 8

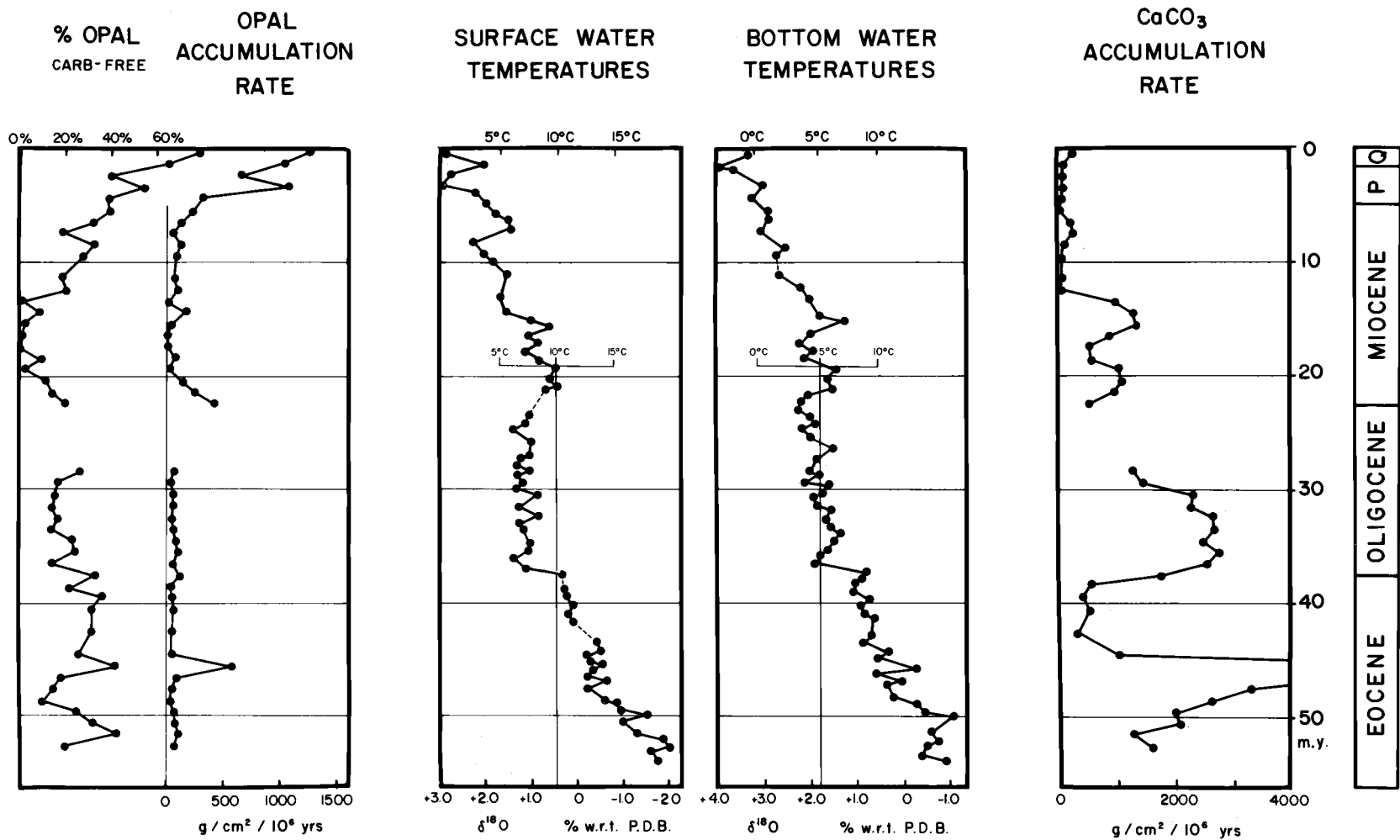


Figure 8. Cenozoic paleotemperatures of Antarctic surface and bottom water, from Shackleton and Kennett, 1974, compared to % opal (carbonate free), and salt-corrected bulk opal and CaCO₃ accumulation rates for sites 266 and 277. Antarctic opal accumulation appears to have an inverse relationship to surface water temperatures.

shows estimated Southern Ocean surface and bottom water temperatures for the Cenozoic. The major fluctuations of temperature increase in frequency and magnitude in the Neogene, and accumulation and production rates of sediments appear to respond. It is apparent that the major fluctuations in productivity are inversely related to temperature (Figure 8). Note especially the relation between carbonate-free opal content and surface temperature.

If productivity is more prolific during periods of relatively cold water, then it must follow that upwelling likewise intensifies during cold periods. This is indeed the case, because upwelling in the Southern Ocean is controlled by two factors, both of which intensify with climatic cooling:

- (1) The intensity of westerly winds which drive surface waters from the Circum-Antarctic Current away from Antarctica, causing a mass deficit near the continent (Hayes et al., 1976; Zillman, 1972; Gordon, 1971b).
- (2) The volume production of AABW which controls global thermohaline circulation (Kemp et al., 1975; Jacobs et al., 1970; Craig and Gordon, 1965; Kennett, in press).

Glaciation can strengthen upwelling by generating intensified atmospheric circulation; sharp temperature gradients between equatorial and glaciated polar regions cause wind velocities to accelerate. These strong westerlies then drive Antarctic Surface Water northeastward,

causing the upwelling of deep, nutrient-rich water to increase. Because opal accumulation has a more direct inverse relationship to surface water temperature than to bottom water temperature, wind-driven circulation should have greater control over upwelling than the production of AABW.

Although AABW production may not be the main control on Southern Ocean upwelling, it is still quite significant. As the volume of shelf ice expands during glacial times, and Antarctic Surface Water cools, AABW production increases, and flow rates accelerate. As the AABW penetrates northward during glacial times, its velocity may reach and exceed erosional capacity, causing a higher frequency of hiatuses associated with bottom water erosion, as is indeed observed (Kennett and Shackleton, 1976; Kennett and Brunner, 1973; Watkins and Kennett, 1972; 1971). Accelerated bottom water in turn serves to speed up thermohaline oceanic turnover, which includes the intensification of upwelling south of the Polar Front (Kemp et al., 1975; Gordon, 1971b).

Further evidence for the association between productivity and low temperature is the relationship between opal production and the amount of ice-rafted terrigenous clay and quartz. In the Neogene, both generally increase during times of cooling (Kennett and Watkins, 1976; Margolis and Kennett, 1971). An exception to this occurs in the Quaternary, when opal production is so high that it dominates the

other sedimentary constituents. During this time, the accumulation of ice-rafted debris decreases while productivity rises. The decreasing non-biogenic accumulation rate in the Quaternary results from the fact that for the last few million years, most of the icebergs have formed offshore, without ever coming into contact with terrigenous matter, and therefore carry only a small sediment load (Warnke, 1970). In addition, very little of the easily erodable, weathered material is left on Antarctica, after tens of millions of years of glacial erosion (Warnke, 1970).

It is clear (Figure 8) that glacial conditions in the Paleogene were not likewise accompanied by increased surface productivity. In particular, the sharp drop in temperature 38 m. y. B. P., while accompanied by a higher input of ice-rafted debris, resulted in only a mild increase in productivity. This absence of a greatly increased opal production 38 m. y. B. P. can be related to the stage of development of oceanic conditions in the Southern Ocean, and perhaps also to the relative location of site 277. First, Southern Ocean water masses were only just beginning to evolve distinguishable identities at that time, the Polar Front did not exist (Kennett, in press), and although AABW was being produced, thermohaline circulation was still only primitive. Atmospheric circulation must have intensified with the onset of glaciation, but without a Circum-Antarctic Current, upwelling could not increase significantly. However, the only evidence

comes from site 277, which may have been north of the upwelling zone adjacent to Antarctica; thus the available evidence may not be representative.

Explaining surface productivity in terms of increased rates of upwelling during cold periods emphasizes the fact that productivity is rate-controlled. It is not the cycling of the seawater itself which controls productivity, but, specifically, the overturn kinetics of the silica cycle (Figure 7) which is imprinted upon circulation patterns. No change is required in the silica cycle itself for increased productivity, other than the accelerated input rate of nutrients, silicic acid in particular. Planktonic silica fixation depends on the rate of supply of silicic acid to the surface (Paasche, 1973). The process of silica fixation can be described using the Michaelis-Menton equation (for enzyme kinetics) in which the rate of silicic acid uptake by plankton is dependent upon the external substrate concentration of by plankton is dependent upon the external substrate concentration of silicic acid:

$$V = V_{\max} \frac{S}{K_t + S} \quad (\text{Nelson et al. , 1976})$$

where S = external substrate concentration of silicic acid

V = specific rate of Si uptake

V_{\max} = maximum specific rate of Si uptake

K_t = substrate concentration of silicic acid when $V = V_{\max}/2$.

This merely shows that the uptake rate for silica is a function of the

external substrate silica concentration, S . Thus, accelerated upwelling allows a concomitant speeding-up of the silica cycle, and supplies more silica to the surface waters, thereby increasing substrate concentration S , and intensifying the rate of surface production.

Having established some of the controls of Neogene surface productivity, fluctuations in productivity can next be discussed.

The times of greatest surface productivity in the Neogene were at the beginning of the Miocene, about 23 m. y. a., again about 14 m. y. a., and after about 8 m. y. a. The reason for the 23 million year peak is not known. Productivity diminished as a brief warming period followed in the Early Miocene, about 20 m. y. a. Surface productivity increased again 14 m. y. a. At this time, Antarctic ice volume expanded, and permanent ice caps developed on the continent (Savin et al., 1975). As temperatures dropped, accumulation of ice-rafted material reached a maximum. By this time, a northward-migrating hydrographic boundary probably very much like the present-day Polar Front separated water masses of distinct characteristics. Thermohaline circulation was fully developed, with upwelling south of the Front (Kennett, in press). By 10 to 12 m. y. B. P., the ice cap on Antarctica was completely developed, causing a northward shift of the Polar Front. This was accompanied by a northward expansion of the Antarctic Surface Water and the siliceous/calcareous boundary between bottom sediments, as well as a northward penetration of

ice-rafted material. From about 22 to 5 m. y. B. P. the Polar Front maintained a constant position about 300 km south of the Southeast Indian Ocean Ridge crest, indicating that the Front was migrating north at a rate comparable to the rate of northward ridge migration (Kemp et al., 1975). An abrupt change near 12 m. y. B. P. from high calcium carbonate content and accumulation to high opal content and accumulation at site 266 records the time when the Polar Front passed over site 266 (Figures 3 and 5). Surface productivity remained fairly constant for a few million years after the crossing. About 8 m. y. B. P., it decreased, most likely due to a temporary warming period at that time (Figure 7). From then to about 5 m. y. B. P. productivity steadily increased, as Late Miocene temperatures steadily decreased. At the Miocene/Pliocene boundary, the Antarctic ice sheet almost doubled in volume (Mayewski, 1975), as temperatures dropped. This caused the Polar Front to advance northward about 300 km to a position coincident with the SE Indian Ocean Ridge crest (Kemp et al., 1975). Surface productivity was immense. Terrigenous accumulation experienced a similar peak. The Late Miocene cooling was felt world-wide (Mayewski, 1975; Casey, 1972; Ingle, 1967). Massive sea ice formation lowered sea level and probably was responsible for the isolation of the Mediterranean Basin (Mayewski, 1975). A brief warm pulse about 4 m. y. B. P. interrupted surface productivity temporarily. Ice retreated at this

time, and sea level rose (Kennett, in press). Thereafter, Antarctic climate continued to deteriorate, and surface productivity increased. From the Quaternary to present, oceanic turnover has reached a maximum intensity due to steep temperature gradients between polar and equatorial regions. Accelerated water mass flow is reflected by vigorous upwelling south of the Polar Front Zone, widespread seafloor erosion (Kennett, in press), and prolific biological productivity in Antarctic Surface Waters.

Calcium Carbonate Preservation

Eocene-Oligocene carbonate accumulation at site 277 is lowest during warmer periods, and highest during colder periods, such as the one beginning 38 m. y. B. P. This time-distribution of CaCO_3 at site 277 is consistent with the theory which suggests that corrosive respiratory CO_2 accumulated in the relatively stagnant bottom waters of warmer times. Prolonged contact of CO_2 -laden bottom water with calcareous sediments causes extensive dissolution (van Andel et al., 1975; Berger, 1970). Conversely, cold periods of pronounced bottom water production clean out CO_2 from bottom waters, thereby increasing preservation. Although this theory may explain the accumulation pattern of CaCO_3 for Paleogene sediments at site 277, it does not explain the Neogene accumulation of CaCO_3 at site 266. Comparing the bottom water temperature curve with calcareous accumulation rate,

during the Neogene (Figure 8), it is evident that colder times were characterized by low CaCO_3 accumulation. Since productivity was higher during colder times, calcium carbonate production must likewise have been higher, and CaCO_3 preservation must have been minimal. Warmer times are manifested by increased preservation of CaCO_3 . Evidently some new process appeared during colder periods in the Neogene that is conducive to carbonate dissolution. It is proposed here that the rate of Southern Ocean upwelling, which became established during the Neogene, influences the preservation or dissolution of calcium carbonate.

Cold oceanic waters have a higher capacity for dissolved CO_2 than relatively warmer waters (Broecker, 1974). Antarctic Bottom Water is by far the coldest water mass, and contains high concentrations of CO_2 (Gordon, 1971b). During cold times the CO_2 content of polar waters increases even further. AABW production increases, thus sending relatively faster-flowing corrosive bottom waters northward, permitting the extensive dissolution of CaCO_3 at the seafloor. In addition, intensified oceanic turnover increases upwelling of Circumpolar Deep Water, which is formed from the deep waters of all oceans (Gordon, 1971b). These waters when they return to the Southern Ocean, contain dissolved CO_2 from respiration in the other oceans. As upwelling accelerates, the supply rate of CO_2 to the surface increases. This would effectively raise the CCD and cause

dissolution higher in the water column. Similarly, intensified overall circulation during glacial times might cause some upwelling of AABW, and supply even more CO_2 to the upper portions of the water column. Thus, like productivity, the preservation or dissolution of CaCO_3 can be considered a rate-controlled process, where kinetics of oceanic turnover are as important as CO_2 concentration.

Surface Productivity in the Antarctic and Pacific Oceans

During the Eocene and Oligocene, productivity in both the Pacific (Leinen, 1976; and in prep), and Antarctic was of comparable magnitude, producing somewhere between 2000 and 7000 g opal/cm²/m. y. In both regions, productivity was high during the Mid-Eocene, although the magnitude of the Antarctic peak is probably much too high. The similarity of these two curves is not surprising, because the same more or less homogeneous Pacific water mass influenced sedimentation in both areas. The Subantarctic and Antarctic water masses, which were beginning to evolve, were located near the Antarctic continent. Thus the developing Antarctic siliceous belt was far south of site 277, and had no influence of sedimentation in the north.

In the Miocene, however, the major trends of the curve appear to be inversely related. The most striking example of this occurs 5 m. y. B. P. , when a dramatic drop in Pacific surface productivity

EXTRAPOLATED SURFACE PRODUCTION OF OPAL

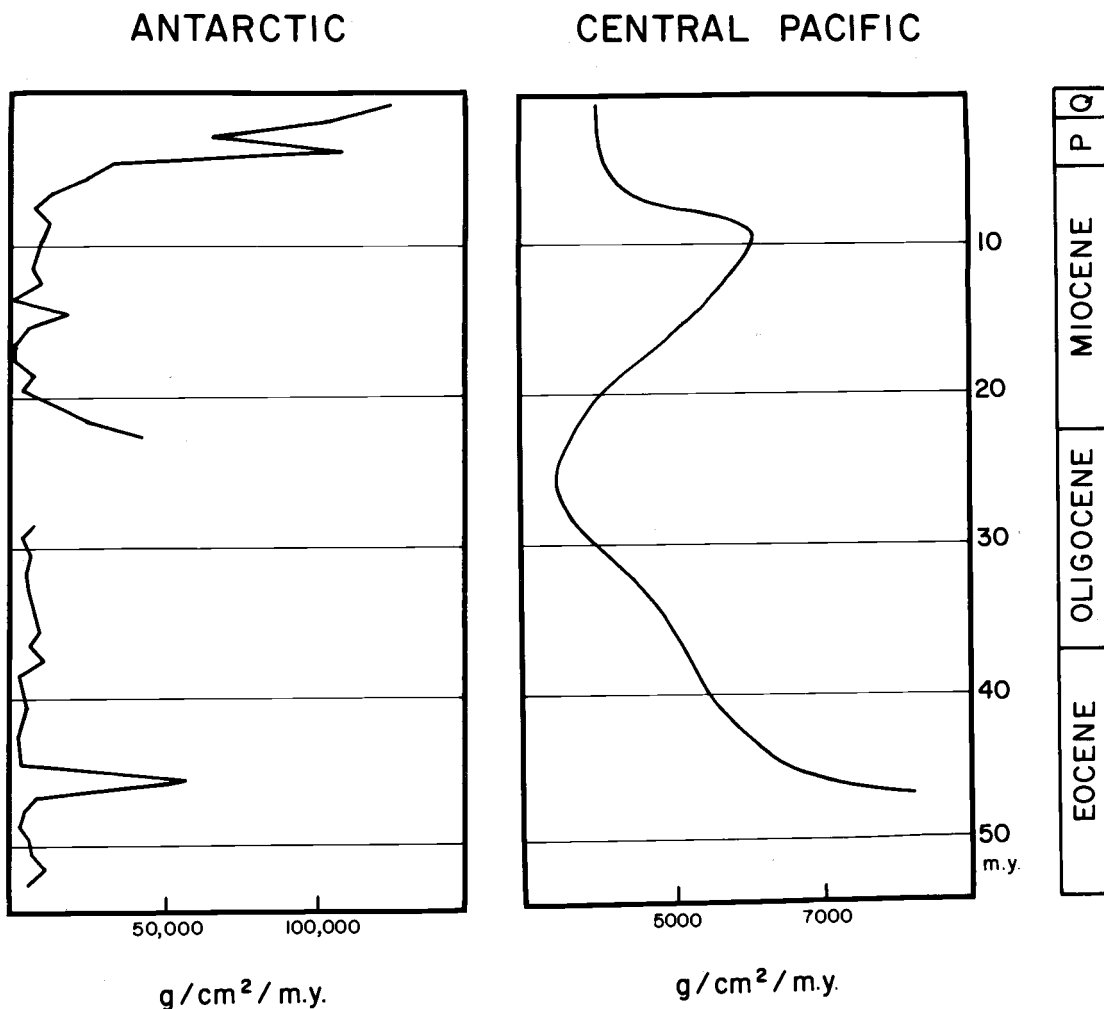


Figure 9. Extrapolated surface production in the Antarctic and Pacific (Leinen, 1977; and in prep.). Oceans for the Cenozoic, assuming a constant rate of silica dissolution throughout the Cenozoic.

is accompanied by an increase of even greater magnitude in Antarctic productivity. It may be possible to explain post-Oligocene patterns in productivity in terms of some sort of "competition" for silica between oceans. Dissolved silica from all oceans travels in deep currents to the Southern Ocean, where it upwells along with other nutrients. Once available, dissolved silica in the surface is assimilated by plankton, and about 80% of the silica is henceforth retained in the biological cycle (Figure 7) (Heath, 1974). As greater amounts of silica are supplied to the Southern Ocean, more and more enters this biological cycle at the expense of other productive oceanic regions. Indeed, the Southern Ocean might be described as a silica trap (Edmond, 1973; Calvert, 1968).

The Southern Ocean can thus be thought of as a silica sink, bound by a semi-permeable hydrographic boundary which admits abundant silica, but allows only a limited amount of silica out via Antarctic Intermediate Water, or AABW. As the Antarctic and Subantarctic Surface Water masses developed, and the Polar Front became established, the Southern Ocean became progressively more a quasi-closed system; hence, the dramatic drop in Pacific opal production towards the end of the Miocene. Similarly, as thermohaline circulation became better established, it could supply higher concentrations of essential nutrients to the Antarctic which could then more efficiently support surface productivity.

Controls on this silica competition are speculative. Since upwelling controls the kinetics of silica supply to Southern Ocean surface waters, it may similarly govern the efficiency with which the Southern Ocean retains its silica. Again, climate would be the ultimate control, possibly allowing a greater percent of the incoming silica to escape during warmer periods.

CONCLUSIONS

(1) It is evident that the most important control on surface productivity in the Southern Ocean is climate. Four periods of increased surface productivity occurred in the Cenozoic. These periods are the Middle Eocene, the beginning of the Miocene, the Middle Miocene, and the Late Miocene/Early Pliocene. The latter period of surface productivity was the most intense, and has persisted for the last 5 million years. Neogene opal production intensifies during glacial periods due to stronger upwelling resulting from accelerated atmospheric circulation and increased production of AABW.

(2) Surface production can be considered to be kinetically controlled, since it is a function of the turn-over rate of the ocean's silica cycle.

(3) The opal production data also confirm the conclusions from previous studies which relate surface productivity indirectly to the tectonic evolution of an ocean basin and to consequent changing circulation patterns. As Antarctica became more isolated, along with the Antarctic Surface Water mass, the Southern Ocean became more conducive to surface productivity. Efficiency has progressed to such an extent that much of the global silica supply has been transferred to the Southern Ocean at the expense of other productive regions such as the Central Equatorial Pacific.

(4) Finally, the Antarctic illustrates the difficulty of applying a general global silica budget, such as the one developed by Wollast (1974), to a specific oceanic region. Instead, in determining the silica budget and silica cycle for a local oceanic province, environmental parameters active in that particular region must be considered. An interplay of chemical, physical, biological, and geological features unique to an ocean basin may significantly effect the dissolution, preservation, and accumulation of biogenic silica.

REFERENCES

- Andrews, P. B., V. A. Gostin, M. A. Hampton, S. V. Margolis, and A. T. Ovenshine, 1974. Synthesis of sedimentation in the Southwest Pacific Ocean, Southwest Indian Ocean, and South Tasman Sea, in Kennett, Houtz, et al., Initial Reports of the Deep Sea Drilling Project, v. 29. Washington, U. S. Gov't Printing Office, p. 1147-1153.
- Arrhenius, G, 1952. Properties of the sediment and their distribution, Reports of the Swedish Deep Sea Exp., v. 5, p. 6-91.
- Badger, R. G., R. D. Gerard, W. E. Benson, H. M. Bolli, W. W. Hay, W. T. Rothwell, Jr., M. H. Ruef, W. R. Riedel, and F. L. Sayles, 1970. Initial Reports of the Deep Sea Drilling Project, v. 4. Washington, D. C., U. S. Gov't Printing Office, 753 p.
- Barker, P. F. and J. Burrell, 1976. The opening of Drake Passage, Proc. Joint Ocean. Assem. Edinburgh, p. 103.
- Berger, W. H., 1970. Planktonic Foraminifera: selective solution and the lysocline, Marine Geology, v. 8, p. 111-138.
- _____, 1970b. Biogenic deep-sea sediments: fractionation by deep sea circulation, Geol. Soc. Amer. Bull., v. 81, p. 1385-1396.
- Bernas, B., 1968. A new method for decomposition and comprehensive analysis of silicates by atomic absorption spectrometry. Anal. Chem., v. 40, p. 1682-1684.
- Bostrom, K., and D. E. Fisher, 1971. Volcanogenic uranium, vanadium, and iron in Indian Ocean sediments, Earth and Planetary Sci. Letters, v. 11, p. 95-98.
- _____, O. Joensuu, S. Valdes, and M. Riera, 1972. Geochemical history of South Atlantic Ocean sediments since the Late Cretaceous, Marine Geology, v. 12, p. 85-122.
- Broecker, W. S., 1974. Chemical Oceanography, Harcourt, Brace and Jovanovich, New York, 214 pp.

- Burkholder, P. R., and L. M. Burkholder, 1967. Primary productivity in surface waters of the South Pacific Ocean, *Limnol. Oceanog.*, v. 12, no. 4, p. 606-617.
- Callahan, J. E., 1971. Velocity structure and heat flux of Antarctic circumpolar current south of Australia, *Journ. Geophys. Res.*, v. 76, no. 24, p. 5859.
- Calvert, S. E., 1968. Silica balance in the ocean and diagenesis, *Nature*, v. 219, p. 219-220.
- _____, 1966. Accumulation of diatomaceous silica sediments in the Gulf of California, *Geol. Soc. Amer. Bull.*, v. 77, p. 569-596.
- Casey, R. E., 1972. Neogene radiolarian biostratigraphy and paleotemperatures, the experimental Mohole Antarctic core E 14-8, *Paleogeography, Paleoclimatology, Palaeoecology* v. 12, p. 115.
- Chen, Pei-Hsin, 1975. Antarctic Radiolaria, *in* Hayes, Frakes et al., *Initial Reports of the Deep Sea Drilling Project*, v. 28. Washington, D. C., U. S. Gov't Printing Office, p. 437-513.
- Chester, R. and H. Elderfield, 1968. The infrared determination of opal in siliceous deep sea sediments. *Geochim. Cosmochim. Acta* v. 32, p. 1128-1140.
- Ciesielski, P. F., 1975. Biostratigraphy and paleoecology of Neogene and Oligocene silicoflagellates from cores recovered during Antarctic Leg 28, DSDP, *in* Hayes, Frakes et al., *Initial Reports of the Deep Sea Drilling Project*, v. 28. Washington, D. C., U. S. Gov't Printing Office, p. 625-692.
- Cook, H. E., I. Zimmels, and J. C. Matti, 1975. X-ray mineralogy data, Austral-Antarctic region, Leg 28, D. S. D. P. *in* Hayes, Frakes, et al., *Initial Reports of the Deep Sea Drilling Project*, v. 28. Washington, U. S. Gov't Printing Office, p. 981-998.
- _____, I. Zimmels, and J. C. Matti, 1974. X-ray mineralogy data, Campbell Plateau and Southern Tasman Sea, *in* Kennett, Houtz, et al., *Initial Reports of the Deep Sea Drilling Project*, v. 29. Washington, U. S. Gov't Printing Office, p. 1173-1186.

- Craig, H. and A. L. Gordon, 1965. Isotopic oceanography: deuterium and oxygen 18 variations in the ocean and the marine atmosphere, *Occ. Pub. Narragansett Mar. Lab.*, v. 3, p. 277-374.
- Cranwell, L. M., H. J. Harrington, and I. G. Spenden, 1960. Lower Tertiary microfossils from McMurdo Sound, Antarctica, *Nature London*, v. 186, p. 700.
- Deer, W. A., R. A. Howie, and J. Zussman, 1971. *An Introduction to the Rock Forming Minerals*, William Clowes and Sons, London, 528 pp.
- Devereaux, I., 1967. Oxygen isotope paleotemperature measurements on New Zealand Tertiary fossils, *New Zealand Jour. Sci.*, v. 10, p. 988-1011.
- Edmond, J. M., 1975. Geochemistry of the circumpolar current, *Oceanus (W. H. O. I.)*, v. 18, no. 4, p. 36-39.
- _____, 1973. The silica budget of the Antarctic circumpolar current, *Nature*, v. 241, p. 391-393.
- Ellis, D. B., 1972. Holocene sediment of the South Atlantic Ocean: the calcite compensation depth and concentration of calcite, opal, and quartz, Master's thesis, Oregon State University, 77 numbered leaves.
- Fletcher, J. O., 1969. Ice extent on the Southern Ocean and its relation to world climate, *in* *Natl. Sci. Found. Memorandum R17-3793*: Santa Monica Ca., The Rand Corp.
- Goldberg, E. D., 1958. Determination of opal in marine sediments, *Jour. Mar. Res.*, v. 17, p. 178-182.
- Gordon, A. L., 1972. Introduction: Physical Oceanography of the Southeast Indian Ocean, *in* Hayes, D. E., ed., *Antarctic Oceanology II: The Australian-New Zealand Sector*, Antarctic Res. Ser., Amer. Geophys. Union, Washington, D. C., v. 19, p. 3-9.
- _____, 1971a. Recent physical oceanography studies of Antarctic waters, *in* Quam, L., ed., *Antarctic Research*, American Assoc. for the Advancement of Sci., Washington, D. C., p. 609-629.

- Gordon, A. L. , 1971b. Oceanography of Antarctic waters, in Reid, ed. , Antarctic Oceanography, v. 15, p. 169-203.
- Hashimoto, I. , and M. L. Jackson, 1960. Rapid dissolution of allophane and kaolinite-halloysite after dehydration. in Proc. of the 7th Nat. Conf. on Clays and Clay Min. , Washington, D. C. , Pergamon Press, p. 102, 113.
- Hayes, D. E. , 1972. Introduction: Marine geophysics of the Southeast Indian Ocean, in Hayes, D. E. , ed. , Antarctic Oceanology II: the Australian-New Zealand Sector, Antarctic Res. Ser. , Amer. Geophy. Union, Washington, D. C. , v. 19, p. 119-124.
- Hayes, D. E. , L. A. Frakes, P. J. Barrett, D. A. Burnes, P. H. Chen, A. B. Ford, A. G. Kaneps, E. M. Kemp, D. W. McCollum, D. J. Piper, R. E. Wall, and P. N. Webb. 1975. Initial Reports of the Deep Sea Drilling Project, v. 28. Washington, D. C. , U. S. Gov't Printing Office, 1017 pp.
- _____, and L. A. Frakes, 1975. General Synthesis, D.S. D.P. Leg 28, in Hayes, Frakes et al. , Initial Reports of the Deep Sea Drilling Project, v. 28. Washington, D. C. , U. S. Gov't Printing Office, p. 919-942.
- _____, and J. Ringis, 1973. Seafloor spreading in the Tasman Sea, Nature, v. 243, p. 454-458.
- Hays, J. D. , J. A. Lozano, N. Shackleton, and G. Irving, 1976. Reconstruction of the Atlantic and western Indian Ocean sectors of the 18,000 B. P. Antarctic Ocean, in Cline, R. M. , and J. D. Hays, eds. , Investigation of Late Quaternary Paleoceanography and Paleoclimatology, Geol. Soc. Amer. Memoir 145, p. 337-374.
- Hays, J. D. , H. E. Cook III, D. G. Jenkins, F. M. Cook, J. T. Fuller, R. M. Goll, E. D. Milow, and W. N. Orr, 1972. Initial Reports of the Deep Sea Drilling Project, v. 9. Washington, D. C. , U. S. Gov't Printing Office, 1205 pp.
- _____, and N. D. Opdyke, 1967. Antarctic radiolaria, magnetic reversals, and climatic change, Sci. , v. 58, p. 1001.
- Heath, G. R. , in press. Processes controlling siliceous biogenous deposits, in Seibold, E. and W. R. Riedel, eds. , Marine plankton and sediments, Third Planktonic Conf. , Kiel.

- Heath, G. R., 1974. Dissolved silica in deep-sea sediments, in Hay, W. W., ed., Soc. Econ. Paleont. and Mineral. Spec. Pub. no. 20, p. 77-93.
- _____, and J. Dymond, in press. Genesis and transformation of metalliferous sediments from the East Pacific Rise, Bauer Deep, and Central Basin, NW Nazca Plate, Geol. Soc. Amer. Bull.
- _____, and J. Dymond, 1973. Interstitial silica in deep sea sediments from the North Pacific, *Geology*, v. 1, p. 181-184.
- _____, and C. Culberson, 1970. Calcite: degree of saturation, rate of dissolution, and the compensation depth in the deep ocean, *Geol. Soc. Amer. Bull.*, v. 81, p. 3157-3160.
- Houtz, R. E., 1974. South Tasman Basin and borderlands: a geophysical summary, in Kennett, Houtz, et al., Initial Reports of the Deep Sea Drilling Project, v. 29. Washington, D. C., U. S. Gov't Printing Office, p. 1135-1146.
- Hurd, D. C. 1974. Interactions of biogenic opal, sediments, and seawater in the Central Equatorial Pacific, *Geochim. Cosmochem. Acta*, v. 37, p. 2257-2282.
- Hurd, D. C., 1972. Interactions of biogenic opal, sediments, and seawater in the Central Equatorial Pacific, Ph. D. thesis, University of Hawaii, Honolulu, 81 numbered leaves.
- Ingle, J. C., Jr., 1973. Summary comments on Neogene biostratigraphy, physical stratigraphy and paleo-oceanography in the marginal northeastern Pacific Ocean, in Kulm, Von Huene et al., Initial Reports of the Deep Sea Drilling Project, v. 18. Washington, D. C., U. S. Gov't Printing Office, p. 949-960.
- Jacobs, M. B., 1974. Clay mineral changes in Antarctic deep sea sediments and Cenozoic climatic events, *Jour. Sed. Petr.*, v. 44, no. 4, p. 1079-1086.
- Jacobs, S. S., A. F. Amos, and P. M. Burckhausen, 1970. Ross Sea oceanography and Antarctic bottom water formation, *Deep Sea Res.*, v. 17, p. 935-962.
- Johnson, D. A., 1974. Deep Pacific circulation: intensification during the early Cenozoic, *Mar. Geol.*, v. 17, p. 71-78.

- Johnson, D. A., 1972. Ocean-floor erosion in the Equatorial Pacific, *Geol. Soc. Amer. Bull.*, v. 83, p. 3121-3144.
- _____, 1971. A model of intensified sea floor erosion during glacial stages (abstract), *EOS trans. Amer. Geophys. Union*, v. 52, no. 4, p. 224.
- Johnson, T. C., 1976. Biogenic opal preservation in pelagic sediments of a small area in the eastern tropical Pacific, *Geol. Soc. Amer. Bull.*, v. 87, p. 1273-1282.
- _____, 1975. The dissolution of siliceous microfossils in deep sea sediments, Ph.D. thesis, Scripps Insti. Oc., Univ. Ca. at San Diego, 163 numbered leaves.
- Jones, M. M., and R. M. Pytcowicz, 1973. Solubility of silica in seawater at high pressures, *Bull. de la Soc. de Liege*, v. 45, p. 125-127.
- Kamatani, A., and H. Oda, in press. Determination of biogenic silica in marine sediments by alkaline solution, *Deep Sea Res.*
- Kaneps, A. G., 1975. Cenozoic planktonic Foraminifera from Antarctic deep sea sediments, Leg 28, DSDP, in Hayes, Frakes et al., *Initial Reports of the Deep Sea Drilling Project*, v. 28. Washington, D. C., U. S. Gov't Printing Office, p. 573-589.
- Kemp, E. M., and P. J. Barrett, 1975. Antarctic glaciation and Early Tertiary vegetation, *Nature*, v. 258, p. 507.
- Kemp, E. M., L. A. Frakes, and D. E. Hayes, 1975. Paleoclimatic significance of diachronous biogenic facies, Leg 28, D. S. D. P., in Hayes, Frakes, et al., *Initial Reports of the Deep Sea Drilling Project*, v. 28. Washington, D. C., U. S. Gov't Printing Office, p. 909-917.
- Kennett, J. P., in press. Cenozoic evolution of Antarctic glaciation, the Circum-Antarctic Ocean, and their impact on global paleoceanography, *Jour. Geoph. Res.*
- _____, and N. J. Shackleton, 1976. Oxygen isotopic evidence for the development of the psychrosphere 38 m. y. ago, *Nature*, v. 260, 1. 513.

Kennett, J. P., and N. D. Watkins, 1976. Regional deep sea dynamic processes recorded by Late Cenozoic sediments of the Southeastern Indian Ocean, *Geol. Soc. Bull.*, v. 87, p. 321-339.

_____, Houtz, R. E., P. B. Andrews, A. R. Edwards, V. A. Gostin, M. Hajos, M. A. Hampton, D. G. Jenkins, S. V. Margolis, A. T. Ovenshine, and K. Perch-Nielsen, 1974. Initial Reports of the Deep Sea Drilling Project, v. 29. Washington, D. C., U. S. Gov't Printing Office, 1197 pp.

_____, Houtz, R. E., P. B. Andrews, A. R. Edwards, V. A. Gostin, M. Hajos, M. A. Hampton, D. G. Jenkins, S. V. Margolis, A. T. Ovenshine, and K. Perch-Nielsen, 1974a. Cenozoic paleoceanography in the Southwest Pacific Ocean, Antarctic glaciation, and the development of the Circum-Antarctic Current, *in* Initial Reports of the Deep Sea Drilling Project, v. 29. Washington, U. S. Gov't Printing Office, p. 1155-1169.

_____, Houtz, R. E., P. B. Andrews, A. R. Edwards, V. A. Gostin, M. Hajos, M. A. Hampton, D. G. Jenkins, S. V. Margolis, A. T. Ovenshine, and K. Perch-Nielsen, 1974b. Development of the Circum-Antarctic Current, *Sci.*, v. 186, p. 144-147.

_____, and C. A. Brunner, 1973. Antarctic Late Cenozoic glaciation: evidence for initiation of ice rafting and inferred increased bottom water activity, *Geol. Soc. Amer. Bull.*, v. 84, p. 2043-2052.

_____, R. E. Burns, J. E. Andrews, M. Churkin, T. A. Davies, P. Dumitrica, A. R. Edwards, J. S. Galehouse, G. H. Packham, and G. J. van der Lingen, 1972. Australian-Antarctic continental drift, paleocirculation changes, and Oligocene deep sea erosion, *Nature Phys. Sci.*, v. 239, p. 51-55.

Kharkar, D. D., K. K. Turekian, and M. Scott, 1969. Comparison of sedimentation rates obtained by ^{32}Si and Uranium decay series: determination in some siliceous Antarctic cores, *Earth and Planetary Sci. Letters*, v. 6, p. 61-68.

Koblentz-Mishke, O. J., V. V. Volkovskiy, and J. G. Kabanova, 1970. Plankton primary productivity of the world ocean, *in*

- Wooster, W. S., ed., Scientific exploration of the South Pacific, U. S. Nat. Acad. Sci., Washington, D. C., p. 183-193.
- Leinen, M., 1977. A normative calculation for determining opal in deep sea sediments, *Geochimica Cosmochim. Acta*, v. 41 n. 4.
- _____, 1976. Biogenic silica sedimentation in the Central Equatorial Pacific during the Cenozoic, Masters thesis, Oregon State Univ., 136 numbered leaves.
- Lewin, J. C., 1961. The dissolution of silica from diatom walls, *Geochim. Cosmochim. Acta*, v. 21, p. 182-198.
- Lisitzin, A. P., 1971. Distribution of siliceous microfossils in suspension and in bottom sediments, in Funnell, M. N., and W. R. Riedel, eds., The Microplaeontology of Oceans, Cambridge Univ. Press, p. 173-195.
- _____, 1967. Basic relationships in distribution of modern siliceous sediments and their connection with climatic zonation, *Inter. Geol. Rev.*, v. 9, no. 5, p. 631-652.
- _____, 1966. Main regularities in the distribution of recent siliceous sediments and their relation to climate zonality, *Geochem. of silica*, Nauka, Moscow.
- _____, 1963. Bottom sediments of the Antarctic shelf, *Acad. Delta and shallow water marine bottom sediments*. Acad. Sci. (U.S.S.R.), Moscow.
- _____, 1962. Bottom sediments of the Antarctic, in *Antarctic Res.*, Amer. Geophy. Union Mono. 7, 81-88.
- Lowrie, W. and D. E. Hayes, 1975. Magnetic properties of oceanic basalt samples, in *Initial Reports of the Deep Sea Drilling Project*, v. 28. Washington, D. C., U. S. Gov't Printing Office, p. 869-878.
- Luyendyk, B. P., D. Forsyth, and J. D. Phillips, 1972. Experimental approach to the paleocirculation of oceanic surface waters, *Geol. Soc. Amer. Bull.*, v. 83, p. 2649-2664.
- MacKenzie, F. T., and R. M. Garrells, 1966. Chemical mass balance between rivers and oceans, *Amer. Jour. Sci.*, v. 264, p. 507-525.

- Margolis, S. V., and J. P. Kennett, 1971. Cenozoic paleoglacial history recorded in subantarctic deep sea cores, *Amer. Jour. Sci.*, v. 271, p. 1-36.
- _____, and J. P. Kennett, 1970. Antarctic glaciation during the Tertiary, recorded in sub-Antarctic deep sea cores, *Sci.*, v. 170, p. 1085-1087.
- Mayewski, P. A., 1975. Glacial geology and Late Cenozoic history of the Transantarctic Mountains, Antarctica, Ohio State Univ. Inst. of Polar Studies, Report 56.
- McIntyre, D. J., and G. T. Wilson, 1966. Preliminary palynology of some Antarctic Tertiary erratics, *New Zealand Jour. of Botany*, v. 4, p. 315.
- Moberly, R., 1972. Origin of lithosphere behind island arcs with reference to the western Pacific, in Shagam, R., ed., *Studies in earth and space sciences*, Geol. Soc. Amer. Memoir 132, p. 35-56.
- Molina-Cruz, A., in press. The relation of the southern trade winds to upwelling processes during the last 75,000 years, *Quat. Res.*
- _____, 1975. Paleoceanography of the subtropical southeastern Pacific during Later Quaternary: a study of Radiolaria, opal, and quartz contents of deep sea sediments, Masters thesis, Oregon State Univ., 179 numbered leaves.
- Molnar, R., T. Atwater, J. Mammerickx, and S. M. Smith, 1975. Magnetic anomalies, bathymetry, and the tectonic evolution of the South Pacific since the Late Cretaceous, *Geophy. J. R. Astron. Soc.*, v. 40, p. 383-420.
- Muller, G., and G. Gastner, 1971. The "Karbonate-Bombe," a simple device for the determination of the carbonate content in sediments, soils, and other materials, *N. Jb. Miner. Mh. (Stuggart) Jg.* 1971, H.10, p. 466-469.
- Nelson, D. M., J. J. Goering, S. S. Kilham, and R. L. Guillard, 1976. Kinetics of silicic acid uptake and rates of silica dissolution in the marine diatom Thalassiosira Pseudonana, *Jour. of Phycology*, v. 12, no. 2, p. 246-252.

- Paashe, E., 1973. Silicon and the ecology of marine plankton diatoms, II: silicate uptake kinetics in fine diatom species, *Mar. Biol.*, v. 19, p. 262-269.
- Pisias, N., 1976. Late Quaternary sediment of the Pacific Basin: sedimentation rates, periodicities, and controls of carbonate and opal accumulation, in Cline, R. M., and J. D. Hayes, eds., Investigation of Late Quaternary Paleoceanography and Paleoclimatology, Geol. Soc. Amer. Memoir 145, p. 375-392.
- _____, G. R. Heath, and T. C. Moore, 1975. Lag times for oceanic responses to climatic change, *Nature*, v. 256, p. 716-
- Ryther, J. H., 1963. Geographic variations in productivity, in Hill, M. N., ed., *The Sea*, v. 2, Interscience, New York, p. 347-380.
- Savin, S. M., R. G. Douglas, and F. G., Stehli, 1975. Tertiary marine paleotemperatures, *Geol. Soc. Amer. Bull.*, v. 86, p. 1499.
- Schink, D. R., K. A. Fanning, and M. E. Pilson, 1974. Dissolved silica in the upper pore waters of the Atlantic Ocean, *Jour. Geophys. Res.*, v. 79, p. 2243-2250.
- Schrader, H. J., 1971. Fecal pellets: Role in sedimentation of pelagic diatoms, *Science*, v. 174, p. 55-57.
- Sclater, J. C., D. Abbott, and J. Thiede, in press. Paleobathymetry and sediments of the Indian Ocean, *Geol. Soc. Amer. Memoir*.
- Shackleton, N. J., and J. P. Kennett, 1974. Paleotemperature history of the Cenozoic and the initiation of Antarctic glaciation: oxygen and carbon isotope analyses in D. S. D. P. sites 277, 279, and 281, in *Initial Reports of the Deep Sea Drilling Project*, v. 29, Washington, D. C., U. S. Gov't Printing Office, p. 743-755.
- Siever, R., and N. Woodford, 1973. Sorption of silica by clay minerals, *Geochim. Cosmochem. Acta*, v. 26, p. 187-194.
- Sillen, L. G., 1961. The physical chemistry of seawater, in Sears, M., ed., *Oceanography*, Washington Amer. Assoc. Adv. Sci., p. 549-581.

- Till, R. and D. A. Spears, 1969. The determination of quartz in sedimentary rocks using an X-ray diffraction technique, *Clays and Clay Min.*, v. 17, p. 323-327.
- van Andel, Tj. H., 1975. Mesozoic and Cenozoic calcite compensation depth and the global distribution of calcareous sediments, *Earth and Planetary Sci. Letters*, v. 26, p. 187-194.
- _____, J. Thiede, J. G. Sclater, and W. W. Hay, in press. Depositional history of the South Atlantic Ocean during the last 125 million years, *Jour. Geophys. Res.*
- _____, G. R. Heath, and T. C. Moore, 1975. Cenozoic history and paleoceanography of the Central Equatorial Pacific Ocean, *Geol. Soc. Amer. Memoir* 143, 134 pp.
- Veevers, J. J., 1974. Western margin of Australia, in Burk, C. A., and C. L. Drake, eds., *The Geology of Continental Margins*, New York, Springer-Verlag Inc., p. 605-616.
- Warnke, D. A., 1970. Glacial erosion, ice rafting, and glacial marine sediments: Antarctica and the Southern Ocean, *Amer. Jour. Sci.*, v. 269, p. 279-294.
- Watkins, N. D. and J. P. Kennett, 1971. Antarctic Bottom Water: major change in velocity during the Late Cenozoic between Australia and Antarctica, *Sci.*, v. 73, p. 813-818.
- Watkins, N. D. and J. P. Kennett, 1972. Regional sedimentary discontinuities and Upper Cenozoic changes in bottom water velocities between Australia and Antarctica, in Hayes, D. E., ed., *Antarctic Oceanology II: the Australian-New Zealand sector*, Antarctic Res. Ser., Amer. Geophys. Union, Washington, D. C., v. 19, p. 273-294.
- Weaver, C. E. and L. D. Pollard, 1973. The chemistry of clay minerals, in *Developments in Sedimentology*, Amsterdam, Elsevier, v. 15, 213 pp.
- Weaver, F., 1973. Pliocene paleoclimatic and paleoglacial history of East Antarctica recorded in deep-sea piston cores. *Sedimentological Research Lab., Florida State Univ. Contr.* no. 36.
- Weissel, J. K., 1974. The Australian-Antarctic discordance: new results and implication, *Jour. Geophys. Res.*, v. 79, p. 2579-2587.

- Weissel, J. K., and D. E. Hayes, 1972. Magnetic anomalies in the Southeast Indian Ocean, in Hayes, D. E., ed., Antarctic Oceanology II: the Australia-New Zealand sector, Antarctic Res. Ser., Amer. Geophys. Union. Washington, D. C., v. 19, p. 165-196.
- _____, and D. E. Hayes, 1971. Asymmetric sea floor spreading south of Australia, *Nature*, v. 231, p. 518-522.
- Wollast, R., 1974. The silica problem, in Goldberg, E. D., ed., *The Sea*, v. 5, Interscience, New York, p. 359-392.
- Wyrski, K., 1974b. Sea level and the seasonal fluctuations of the equatorial currents in the Western Pacific Ocean. *Jour. Phys. Oceanog.*, v. 4, p. 91-103.
- Zillman, J. W., 1972. Solar radiation and sea-air interaction, south of Australia, in Hayes, D. E., ed., Antarctic Oceanology II: the Australia-New Zealand sector, Antarctic Res. Ser., Amer. Geophys. Union, Washington, D. C., v. 19, p. 11-40.

APPENDICES

APPENDIX I: METHODS

The technique for determining the opal content in marine sediments for this study follows that of Leinen (1977), but with two modifications. A regression equation different from that formulated for the Pacific is used to predict clay-bound silica in the Southern Ocean, and second, due to the significant input of terrigenous material in high southern latitudes, a greater emphasis is placed on the specific estimation of ice-rafted detrital quartz in as many samples as possible.

Sample Preparation

Two sets of samples were subjected to analytical procedures in this study. The first, main set consists of 45 composite samples, from D. S. D. P. sites 266 and 277. These two sites together form a more or less continuous Cenozoic time sequence in Southern Ocean pelagic sedimentation (Figure 2). Each composite sample consists of from 1 to 8 samples which, when combined, represent a one-million year interval (Appendix II). These 45 samples, spanning from the Recent to 53 m. y. B. P. form the basis for this study, and were used to determine opal accumulation rates.

A second set of 17 samples from D. S. D. P. sites 264A, 226, 277, and 278 contains little to no observable opal in smear slides.

These samples are composed of clay, or carbonate and clay, and they are used to formulate the regression equation that predicts clay-bound silica in each of the 45 samples. The Al, Mg, and Si analytical concentrations determined by Atomic Absorption Spectroscopy (AAS) for these 17 samples were processed by multiple regression analysis in which Si is the dependent variable, and Al and Mg are the independent variables.

Both sets of samples were freeze dried, ground, and put through a sample splitter ten times to homogenize the sediment. Salt content was determined on the basis of water loss (Appendix III), using the relation:

$$\% \text{ salt} = \frac{\% \text{ water loss} \times 0.035}{100 - \% \text{ water loss}}$$

All weight percents are calculated on a salt-free basis.

Weight percent calcium carbonate was determined using the Karbonat Bombe (Muller and Gastner, 1971) for high CaCO_3 samples, and LECO Carbon Analyzer for samples containing less than 25% CaCO_3 (Hays, Cook et al., 1972; Badger, Gerard et al., 1970). Samples were run in duplicate, or until within 2%.

Quartz was determined on samples by X-ray diffraction analysis (Ellis, 1972; Till and Spears, 1969) with an accuracy of $\pm 5\%$ (carbonate-free). If sample volume was insufficient for X-ray analysis, quartz values were interpolated from a plot of the analytical quartz

values, and cross checked with published quartz data from X-ray analyses included in the Initial Reports (Cook et al., 1975; 1974). Quartz determinations for this study are listed in Appendix III.

In the final chemical analysis, 200 to 500 mg of each sample was digested in Teflon-lined steel bombs, at 110° C with aqua regia and hydrofluoric acid. After neutralization with boric acid (Bernas, 1968), the samples were analyzed for Si, Al, and Mg by Atomic Absorption Spectroscopy (AAS). The corresponding chemical data are listed in Appendices V and VI. Samples were run in duplicate, with a precision of 1-2% for Al, Mg, and Si in samples low in CaCO₃, and from 2-5% for samples high in CaCO₃. Comparison with U.S.G.S. standard rock and North Pacific Sediment Standard indicated no systematic error.

From the total silica value for each of the 45 samples (determined by AAS) the following two values were subtracted to obtain opal concentrations:

- the theoretical value for clay-bound silica (as predicted from the equation resulting from the regression analysis
- the quartz value (X-ray diffraction).

The remaining silica fraction is assumed to represent biogenic opal. Biogenic opal values are then used to calculate opal accumulation rates.

Estimation of Clay-Bound Silica

In the 17 selected opal-free samples, the only silica fractions are clay-bound silica, and quartz. The quartz value is subtracted from the total silica value (determined by AAS), and the remaining silica value is that which is specifically associated with clay. This "pure" clay-bound silica value is regressed against Al and Mg concentrations determined for the same 17 samples. The regression attempts to characterize the clay-bound silica in terms of Al and Mg. Different combinations of the five parameters Al, Al², Mg, Mg², and Al×Mg are used in the search for the best model (or equation) to characterize clay-bound silica. The regression analysis associates a coefficient with each parameter in the model, and provides a y-intercept. It also furnishes statistical information describing how closely the equation-predicted clay-bound silica compares to the measured clay-bound silica value. The equation used for Pacific sediments estimates total clay-bound silica, and is in the form:

$$Si_{(\text{non-biog.})} = 4.33 \text{ Al} + 1.36 \text{ Mg}^2 \quad (\text{Leinen, 1977})$$

In this study, the equation providing the best fit to the chemical data is:

$$Si_{(\text{clay-bound})} = 4.54 \text{ Al} - 1.02 \text{ Al} \times \text{Mg} - 1.88$$

This equation was selected from 40 equations, on the basis of

correlation coefficient, T-values, and standard error. This statistical information is listed in Table 1. The residuals between the predicted and measured clay-bound silica are very small (Figure 10), another reason for selecting this particular equation.

The equation is then applied to the Al and Mg values determined analytically by AAS for the 45 composite samples, to predict a clay-bound silica value for each sample. The regression equation predicts slightly negative clay-bound silica values for a few of the 45 samples which contain very little to no clay. This could be due to an error in the detrital quartz correction, or it could be an artifact of the equation for samples with low clay content. In all of these cases, the discrepancy is well within the limits of standard error. The slightly negative values are taken to be zero.

The factor accounting for most of the variance in the equation is Al. The Al×Mg term is not as important, accounting for only 1.6% of the variance. Thus, clay-bound silica in Southern Ocean clays can almost be predicted using a simple Si:Al₂O₃ ratio (Leinen, 1976). Using the additional Al×Mg term improves the model only slightly. This result is consistent with the mineralogy of the Southern Ocean region, which is predominantly illite, having an average SiO₂:Al₂O₃ ratio of 2.50 (Weaver and Pollard, 1973). The SiO₂:Al₂O₃ ratio suggested by the regression equation is 2.26. Illite does not contain Mg⁺² cations, and the presence of interlayer K⁺ cations causes a

Table 1. Statistics of regression equation.

variable name	regression coefficient	std. error of reg. coef.	computed T-values
Al	4.54100	0.53544	8.481
Al × Mg	-1.01633	0.36039	-2.820
intercept	-1.87990		
multiple correlation coefficient		0.986	
standard error of estimate		1.313	

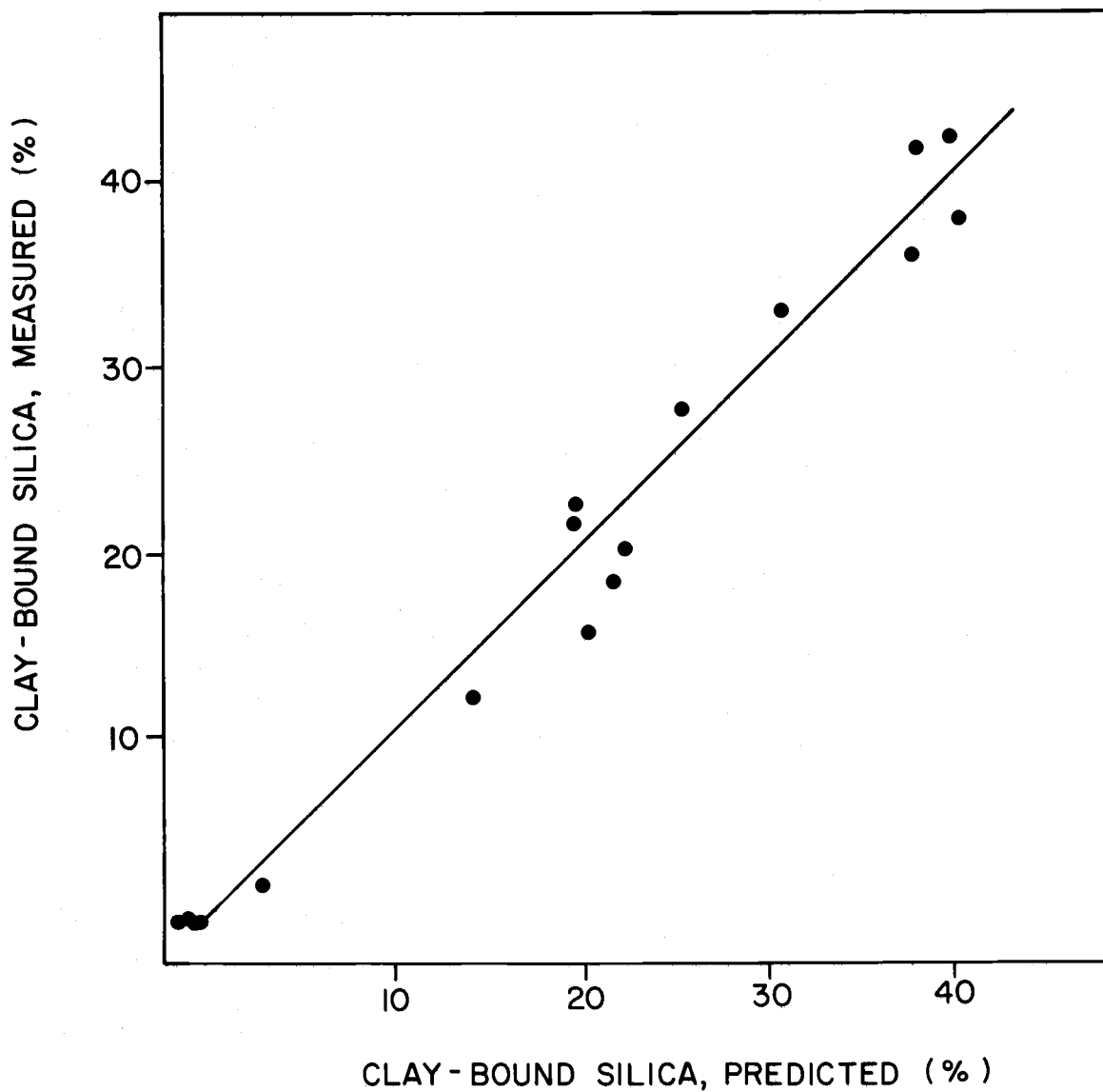


Figure 10. Comparison of clay-bound silica measured in 17 opal-free sediment samples with that predicted by the regression equation described in the text. Diagonal line indicates perfect correspondence between clay-bound silica, predicted and measured.

low cation-exchange capacity (Deer, Howie, and Zussman, 1971).

The $Al \times Mg$ term in the model becomes increasingly important in older samples which contain significant amounts of montmorillonite (Jacobs, 1974). In these, Mg could be important in the prediction of clay-bound silica.

APPENDIX II: Composite Samples and Their Included DSDP Samples

Site	Age Interval (m.y.)	Atomic Abs. Accession #	Depth Interval at site (cm)	DSDP Samples		
				Core	Section	Depth in Section (cm)
266	(0 - 1 m.y.)	PS1851	103-2860	1	2	53-55
				1	4	50-52
				1	3	58-60
266	(1 - 2 m.y.)	PS1852	4522-6802	3	1	122-127
				4	2	51-53
				4	4	50-52
266	(2 - 3 m.y.)	PS1853	8550-8551	5	3	50-51
				5	5	50-51
266	(3 - 4 m.y.)	PS1854	10150-12501	6	1	50-51
				6	5	50-51
				7	1	125-126
				7	4	50-51
266	(4 - 5 m.y.)	PS1855	13002-13451	8	1	52-53
				8	4	50-51
266	(5 - 6 m.y.)	PS1856	14105-14106	9	2	55-56

APPENDIX II: Continued

Site	Age Interval (m.y.)	Atomic Abs. Accession #	Depth Interval at site (cm)	DSDP Samples		
				Core	Section	Depth in Section (cm)
266	(6 - 7 m.y.)	PS1857	14904-15204	10	1	54-55
				10	2	53-54
				10	3	53-54
266	(7 - 8 m.y.)	PS1858	15454-15851	10	4	54-55
				10	5	53-54
				10	6	50-51
				11	1	50-51
266	(8 - 9 m.y.)	PS1859	16000-16301	11	2	50-51
				11	4	50-51
266	(9 -10 m.y.)	PS1860	16575-16676	11	6	25-26
				11	6	125-126
266	(11-12 m.y.)	PS1861	17750-17751	12	1	50-51
266	(12-13 m.y.)	PS1862	17975-18051	12	2	125-126
				12	3	50-51
266	(13-14 m.y.)	PS1863	19677-19678	13	1	77-78

APPENDIX II: Continued

Site	Age Interval (m.y.)	Atomic Abs. Accession #	Depth Interval at site (cm)	DSDP Samples		
				Core	Section	Depth in Section (cm)
266	(14-15 m.y.)	PS1864	19800-22001	13	2	50-51
				13	3	53-54
				13	4	50-51
				13	5	50-51
				13	6	50-51
				14	2	50-52
				14	3	50-51
				14	4	50-51
266	(15-16 m.y.)	PS1865	23450-25954	15	1	50-51
				15	2	50-51
				16	1	50-51
				16	2	50-51
				17	1	95-96
				17	5	53-54
266	(16-17 m.y.)	PS1866	27270-27901	18	1	70-71
				18	2	125-126
				18	4	50-52
				18	5	100-101

APPENDIX II: Continued

Site	Age Interval (m.y.)	Atomic Abs. Accession #	Depth Interval at site (cm)	DSDP Samples		
				Core	Section	Depth in Section (cm)
266	(17-18 m.y.)	PS1867	29125-29901	19	1	25-26
				19	2	125-126
				19	4	50-51
266	(18-19 m.y.)	PS1868	29900-29901	19	6	50-51
266	(19-20 m.y.)	PS1869	31066-31506	20	1	66-67
				20	2	53-54
				20	3	55-56
				20	4	55-56
266	(20-21 m.y.)	PS1870	32935-33704	21	1	25-26
				21	2	125-126
				21	4	53-54
				21	6	53-54
266	(21-22 m.y.)	PS1871	36325-36326	22	4	125-126
266	(22-23 m.y.)	PS1872	37035-37037	23	1	35-37
277	(28-29 m.y.)	PS1873	502-655	1	4	52-53
				1	5	54-55

APPENDIX II: Continued

Site	Age Interval (m.y.)	Atomic Abs. Accession #	Depth Interval at site (cm)	DSDP Samples		
				Core	Section	Depth in Section (cm)
277	(29-30 m.y.)	PS1874	1203-1853	2	2	53-54
				2	5	50-51
				3	2	52-53
277	(30-31 m.y.)	PS1875	2300-4053	3	5	50-51
				4	2	52-53
				4	5	50-51
				5	4	52-53
277	(31-32 m.y.)	PS1876	4703-6751	6	2	53-54
				6	6	51-52
				7	2	52-53
				7	5	50-51
				8	3	50-51
277	(32-33 m.y.)	PS1877	7850-9451	9	4	51-52
				10	2	50-51
				10	4	51-52
				10	6	48-49
				11	2	50-51

APPENDIX II: Continued

Site	Age Interval (m.y.)	Atomic Abs. Accession #	Depth Interval at site (cm)	DSDP Samples		
				Core	Section	Depth in Section (cm)
277	(33-34 m.y.)	PS1878	9250-11951	11	4	50-51
				11	6	48-49
				12	3	51-52
				12	5	50-51
				13	1	59-60
				13	4	53-54
				13	6	50-51
277	(34-35 m.y.)	PS1879	12348-13552	14	2	48-49
				14	5	50-51
				15	2	53-54
				15	4	51-52
277	(35-36 m.y.)	PS1880	14500-16104	16	4	50-51
				17	4	51-52
				17	6	50-51
				18	2	53-54
277	(36-37 m.y.)	PS1881	17051-19101	19	2	51-52
				20	2	51-52
				20	5	50-51
				21	3	50-51

APPENDIX II: Continued

Site	Age Interval (m.y.)	Atomic Abs. Accession #	Depth Interval at site (cm)	DSDP Samples		
				Core	Section	Depth in Section (cm)
277	(37-38 m.y.)	PS1882	19800-20854	22	1	100-101
				22	2	51-52
				23	1	50-51
				23	2	53-54
277	(38-39 m.y.)	PS1883	21000-21001	23	3	50-51
277	(39-40 m.y.)	PS1884	21725-21726	24	1	125-126
277	(40-41 m.y.)	PS1885	21946-21947	24	3	46-47
277	(42-43 m.y.)	PS1886	22750-22751	25	2	50-51
277	(44-45 m.y.)	PS1887	23574-23776	26	1	74-75
				26	2	125-126
277	(45-46 m.y.)	PS1888	24519-29576	27	1	69-70
				28	2	49-50
				30	2	53-54
				30	5	50-51
				32	1	50-51
				32	3	75-76

APPENDIX II: Continued

Site	Age Interval (m.y.)	Atomic Abs. Accession #	Depth Interval at site (cm)	DSDP Samples		
				Core	Section	Depth in Section (cm)
277	(46-47 m.y.)	PS1889	31300-34961	33	2	50-51
				34	1	51-52
				34	2	60-61
				35	1	60-61
277	(47-48 m.y.)	PS1890	35095-37151	35	2	45-46
				36	1	120-121
				36	3	50-51
277	(48-49 m.y.)	PS1891	37951-38901	37	2	51-52
				38	2	50-51
277	(49-50 m.y.)	PS1892	39799-40952	39	1	149-150
				40	1	133-134
				40	3	51-52
277	(50-51 m.y.)	PS1893	41625-41901	41	1	75-76
				41	2	45-46
				41	3	50-51

APPENDIX II: Continued

Site	Age Interval (m.y.)	Atomic Abs. Accession #	Depth Interval at site (cm)	DSDP Samples		
				Core	Section	Depth in Section (cm)
277	(51-52 m.y.)	PS1894	42675-43506	42	2	25-26
				42	2	123-124
				42	3	52-53
				43	1	55-56
277	(52-53 m.y.)	PS1895	43650-43778	43	2	50-51
				43	3	27-28

APPENDIX III: Weight Percent Biogenic and Non-Biogenic Components, salt corrected

Site	Age Interval (m.y.)	% Opal bulk	% carb-free	% CaCO ₃	% Non-biogenic	% Salt	% Detrital Quartz
266	(0 - 1)	69.4	78.1	11.1	19.5	6.1	0.0
	(1 - 2)	64.0	65.4	2.3	33.8	5.4	1.3
	(2 - 3)	38.7	39.5	2.0	59.2	4.9	1.4
	(3 - 4)	53.5	54.5	1.8	44.7	6.2	1.4
	(4 - 5)	38.4	39.3	2.3	59.3	5.4	2.3
	(5 - 6)	38.4	39.2	2.1	59.6	5.1	3.0
	(6 - 7)	21.0	32.7	35.7	43.3	3.1	3.6
	(7 - 8)	11.8	18.6	36.4	51.8	3.2	4.3*
	(8 - 9)	27.4	32.3	15.3	57.3	4.0	4.5
	(9 -10)	28.0	28.3	1.3	70.7	4.4	4.7
	(11-12)	16.5	17.9	7.9	75.6	4.0	5.2
	(12-13)	19.0	19.8	3.9	77.1	4.8	5.7

APPENDIX III (continued)

Site	Age Interval	% Opal bulk	carb-free	% CaCO ₃	% Non-biogenic	% Salt	% Detrital Quartz
266	(13-14)	0.0	0.0	79.5	20.5	2.0	4.8
	(14-15)	5.0	7.8	36.1	59.0	2.9	7.6*
	(15-16)	0.6	1.0	41.2	58.2	2.9	10.6*
	(16-17)	0.01	0.02	48.5	51.5	2.6	9.4*
	(17-18)	0.03	0.05	44.0	56.0	2.5	9.2*
	(18-19)	5.0	9.1	45.2	49.8	2.5	9.4*
	(19-20)	1.0	2.5	59.9	39.1	2.2	6.7*
	(20-21)	5.9	11.2	47.2	46.9	2.3	7.3*
	(21-22)	8.5	13.7	37.4	54.0	2.3	6.2*
	(22-23)	15.8	19.5	19.0	65.2	1.7	5.4
277	(28-29)	3.7	25.5	85.6	10.7	2.4	1.0
	(29-30)	1.6	16.1	90.4	8.0	2.0	1.0

APPENDIX III (continued)

Site	Age Interval	% Opal bulk	carb-free	% CaCO ₃	% Non- biogenic	% Salt	% Detrital Quartz
277	(30-31)	1.7	15.0	88.9	9.4	2.1	1.0*
	(31-32)	1.5	14.6	89.6	8.9	2.0	1.0
	(32-33)	1.4	16.7	91.4	7.1	1.8	1.0
	(33-34)	1.3	14.1	90.6	8.0	1.8	0.9*
	(34-35)	2.6	23.6	89.1	8.3	1.7	1.0
	(35-36)	2.4	24.3	90.3	7.3	1.6	1.0
	(36-37)	1.7	14.7	88.7	9.6	1.8	1.3
	(37-38)	4.3	32.8	87.0	8.8	1.5	1.5*
	(38-39)	3.6	22.1	83.7	12.7	1.4	1.5
	(39-40)	6.7	34.7	80.0	12.5	1.4	1.6
	(40-41)	6.6	32.2	79.4	14.0	1.8	1.6
	(42-43)	5.2	31.4	83.5	11.3	1.1	1.6

APPENDIX III (continued)

Site	Age Interval	% Opal bulk	carb-free	% CaCO ₃	% Non-biogenic	% Salt	% Detrital Quartz
277	(44-45)	3.2	25.7	87.4	9.4	1.5	1.8
	(45-46)	6.6	43.1	84.7	8.7	1.5	1.9*
	(46-47)	1.6	17.5	90.9	7.5	1.2	1.6
	(47-48)	1.2	14.8	91.8	7.0	1.2	1.2
	(48-49)	0.9	10.0	91.3	7.8	1.2	0.8
	(49-50)	1.9	24.7	92.2	5.9	0.9	0.4*
	(50-51)	2.8	31.8	91.3	5.9	1.2	0.4*
	(51-52)	5.5	42.4	87.0	7.5	0.9	0.4*
	(52-53)	3.0	20.3	85.2	11.8	0.8	0.5*

* analytical quartz values from X-ray diffraction

APPENDIX IV: Sedimentation and Accumulation Rates

Accumulation rates in $\text{g/cm}^2/\text{m.y.}$

Sedimentation rates in m/m.y.

Site	Age Interval (m.y.)	Sed. Rate	Bulk Sed. Accum Rate	Opal Accum Rate	CaCO_3 Accum Rate	Non-biog. Accum Rate
266	(0 - 1)	40.0	1797	1240	199	350
	(1 - 2)	30.0	1590	1016	37	537
	(2 - 3)	28.0	1710	666	34	1014
	(3 - 4)	29.0	2005	1073	36	896
	(4 - 5)	11.0	805	305	19	477
	(5 - 6)	8.0	610	232	13	363
	(6 - 7)	7.0	541	114	193	234
	(7 - 8)	7.0	555	65	202	287
	(8 - 9)	5.0	406	110	62	233
	(9 -10)	3.5	288	81	4	204
	(11-12)	4.5	379	61	30	287

APPENDIX IV (continued)

Site	Age Interval	Sed. Rate	Bulk Sed. Accum Rate	Opal Accum Rate	CaCO ₃ Accum Rate	Non-biog. Accum Rate
266	(12-13)	5.5	469	89	18	362
	(13-14)	14.0	1223	0.01	972	251
	(14-15)	36.5	3446	171	1244	2031
	(15-16)	32.5	3199	18	1318	1863
	(16-17)	16.5	1691	0.2	820	871
	(17-18)	11.0	1138	0.3	501	637
	(18-19)	11.5	1231	60	548	604
	(19-20)	16.0	1704	17	1021	666
	(20-21)	20.0	2211	131	1044	1039
	(21-22)	23.0	2566	220	960	1386
	(22-23)	23.0	2612	412	496	1704

APPENDIX IV (continued)

Site	Age Interval	Sed. Rate	Bulk Sed. Accum Rate	Opal Accum Rate	CaCO ₃ Accum Rate	Non-biog. Accum Rate
277	(28-29)	15.0	1522	56	1303	163
	(29-30)	15.0	1552	24	1403	125
	(30-31)	24.5	2585	43	2298	244
	(31-32)	23.4	2539	39	2275	225
	(32-33)	26.0	2900	42	2651	208
	(33-34)	25.5	2922	39	2647	236
	(34-35)	23.5	2811	72	2505	234
	(35-36)	25.0	3066	72	2769	225
	(36-37)	23.0	2868	48	2544	276
	(37-38)	16.0	2027	87	1763	177
	(38-39)	5.0	633	23	530	80
	(39-40)	4.0	510	34	413	64

APPENDIX IV (continued)

Site	Age Interval	Sed. Rate	Bulk Sed. Accum Rate	Opal Accum Rate	CaCO ₃ Accum Rate	Non-biog. Accum Rate
277	(40-41)	5.0	639	42	507	89
	(42-43)	3.0	389	20	325	44
	(44-45)	9.0	1168	38	1021	109
	(45-46)	66.5	8828	582	7477	768
	(46-47)	39.0	5335	85	4850	401
	(47-48)	25.0	3521	43	3232	246
	(48-49)	20.0	2857	25	2609	224
	(49-50)	15.0	2173	42	2004	128
	(50-51)	15.5	2261	63	2064	134
	(51-52)	10.0	1479	81	1287	111
	(52-53)	12.5	1848	55	1575	218

APPENDIX V: Salt-Corrected Chemical Data for 45 Antarctic Samples

Site	Age Interval (m.y.)	% Al (average)	% Mg (average)	% Si (average)
266	(0 - 1)	0.75	4.70	33.60
	(1 - 2)	1.84	0.66	35.72
	(2 - 3)	4.24	1.05	31.59
	(3 - 4)	2.65	0.73	33.86
	(4 - 5)	3.96	1.03	30.98
	(5 - 6)	4.05	1.04	31.58
	(6 - 7)	2.81	0.71	20.34
	(7 - 8)	3.48	0.81	18.59
	(8 - 9)	4.11	1.00	27.55
	(9 -10)	5.88	1.40	31.74
	(11-12)	5.85	1.40	26.51
	(12-13)	5.87	1.39	28.04
	(13-14)	0.89	0.32	4.12
	(14-15)	3.88	0.94	17.94
	(15-16)	3.45	0.90	15.83
	(16-17)	3.07	0.79	14.00
	(17-18)	3.36	0.92	14.55
	(18-19)	3.00	0.81	16.01
	(19-20)	2.19	0.62	10.29
	(20-21)	3.03	0.84	15.46
	(21-22)	4.04	1.32	17.96

APPENDIX V (continued)

Site	Age Interval (m.y.)	% Al (average)	% Mg (average)	% Si (average)
266	(22-23)	5.32	1.87	22.06
277	(28-29)	0.43	0.33	2.21
	(29-30)	0.29	0.22	1.22
	(30-31)	0.24	0.21	1.27
	(31-32)	0.21	0.14	1.18
	(32-33)	0.20	0.14	1.13
	(33-34)	0.21	0.16	1.06
	(34-35)	0.40	0.21	1.64
	(35-36)	0.36	0.18	1.59
	(36-37)	1.25	0.17	1.38
	(37-38)	0.55	0.25	2.70
	(38-39)	0.65	0.28	3.31
	(39-40)	0.94	0.35	5.88
	(40-41)	1.07	0.38	6.41
	(42-43)	0.70	0.26	4.30
	(44-45)	0.51	0.24	2.63
	(45-46)	0.40	0.21	3.98
	(46-47)	0.24	0.18	1.49
	(47-48)	0.22	0.15	1.12
	(48-49)	0.15	0.16	0.78
	(49-50)	0.26	0.22	1.09
	(50-51)	0.37	0.26	1.47
	(51-52)	0.49	0.28	2.98
	(52-53)	0.78	0.33	3.02

APPENDIX VI: Salt-Corrected Chemical Data for 17 Opal-Free Samples

Site	Sample	% Si bulk	% Si opal	% Si qtz	% Si clay-bound opal-free qtz-free	% Al	% Mg
264A	2-3	1.03	0.43	0.60	0.00	0.31	0.17
	3-4	1.02	0.44	0.58	0.00	0.24	0.19
266	14-15	17.94	1.40	3.57	12.97	3.88	0.94
	15-16	15.83	1.40	4.94	9.48	3.45	0.90
	16-17	14.00	1.40	5.25	7.36	3.07	0.79
	17-18	14.55	1.40	4.41	8.74	3.40	0.92
	18-19	16.01	1.40	4.47	10.14	3.00	0.81
	19-20	10.29	1.40	3.19	5.70	2.19	0.62
	20-21	15.46	1.40	3.44	10.62	3.03	0.84
	268	4-1	32.79	0.93	12.31	19.54	5.59
	9-1	31.64	1.87	9.99	19.78	6.31	1.27
	18-1	32.79	0.47	14.61	17.71	6.68	1.39

APPENDIX VI (continued)

Site	Sample	% Si bulk	% Si opal	% Si qtz	% Si	% Al	% Mg
					clay-bound opal-free qtz-free		
268	20-1	32.46	2.80	12.84	16.82	6.51	1.50
277	29-30	1.22	0.70	0.49	0.03	0.29	0.22
	37-38	2.70	2.00	0.70	0.00	0.55	0.25
	52-53	3.02	1.87	0.24	0.91	0.78	0.33
278	8-1	28.87	6.54	6.87	15.46	5.40	1.48